Personalized Itinerary Planner and Abstract Book

AGU 2011 Fall Meeting

December 04 - 09, 2011

To make changes to your intinerary or view the full meeting schedule, visit http://agu-fm11.abstractcentral.com:80

Sunday, December 04, 2011

You have nothing scheduled for this day

Monday, December 05, 2011

Time	Session Info
8:00 AM-12:20 PM, Halls A-C (Moscone South), **T11A. Characterization of Fault Zones by Geophysical Imaging I Posters**	
8:00 AM-12:20 PM	**T11A-2274. Strain localization and crustal thickness variation across major strike slip faults in southern California revealed by receiver function studies** P. Zhang; M.S. Miller; J.F. Dolan; I.W. Bailey; D.A. Okaya
8:00-8:00 AM	**T11A-2279. Characterizing the recent behavior and earthquake potential of the blind western San Cayetano and Ventura fault systems** L.J. McAuliffe; J.F. Dolan; J. Hubbard; J.H. Shaw
8:00 AM-10:00 AM, Room 102 (Moscone South), **IN11D. High-Resolution Modeling in the Geosciences Using GPU and Many-Core Architectures I**	
8:15-8:30 AM	**IN11D-02. A Parallel Simulated Annealing Approach to Solve for Earthquake Rupture Rates** K. Milner; M.T. Page; E.H. Field
8:00 AM-10:00 AM, Room 2009 (Moscone West), **S11D. The Future of Structural Seismology I**	
8:30-8:45 AM	**S11D-03. Seismological Constraints on the Deep Structure of Continents *(Invited)*** T.H. Jordan; E. Paulson
1:40 PM-6:00 PM, Halls A-C (Moscone South), **G13A. Advances in Gravimetry and Geodetic Imaging: Instrumentation, Methods, and Applications III Posters**	
1:40 PM-6:00 PM	**G13A-0872. Rapid Determination of Near-Fault Earthquake Deformation Using LIDAR** A.A. Borsa; J.H. Minster
1:40 PM-6:00 PM, Halls A-C (Moscone South), **IN13A. High-Resolution Modeling in the Geosciences Using GPU and Many-Core Architectures III Posters**	
1:40 PM-6:00 PM	**IN13A-1318. Acceleration of 3D Finite Difference AWP-ODC for seismic simulation on GPU Fermi Architecture** J. Zhou; Y. Cui; D. Choi
1:40 PM-6:00 PM, Halls A-C (Moscone South), **T13A. Creep and Faulting in Nature, the Lab, and Theory I Posters**	
1:40 PM-6:00 PM	**T13A-2350. Detection of repeating and "anti-repeating" earthquakes in the Bucaramanga Nest** S.A. Barrett; G. Prieto; G.C. Beroza

1:40 PM-3:40 PM, Room 2016 (Moscone West), **T13G. Characterization of Fault Zones by Geophysical Imaging II**	
2:40-2:55 PM	**T13G-05. Structure and seismic hazard of the Ventura Avenue anticline and Ventura fault, California** J. Hubbard; J.H. Shaw; J.F. Dolan; T.L. Pratt; L.J. McAuliffe
2:40-2:55 PM	**T13G-05. Structure and seismic hazard of the Ventura Avenue anticline and Ventura fault, California** J. Hubbard; J.H. Shaw; J.F. Dolan; T.L. Pratt; L.J. McAuliffe
4:00 PM-6:00 PM, Room 3022 (Moscone West), **DI14A. Advances in Computational Modelling in Geoscience I**	
5:45-6:00 PM	**DI14A-08. PyLith: A Finite-Element Code for Modeling Quasi-Static and Dynamic Crustal Deformation *(Invited)*** B. Aagaard; C.A. Williams; M.G. Knepley
5:45-6:00 PM	**DI14A-08. PyLith: A Finite-Element Code for Modeling Quasi-Static and Dynamic Crustal Deformation *(Invited)*** B. Aagaard; C.A. Williams; M.G. Knepley

Tuesday, December 06, 2011

Time	Session Info
8:00 AM-12:20 PM, Halls A-C (Moscone South), **S21A. Active Fault Data as Input for Seismic Hazard Analysis (SHA) IV Posters**	
8:00 AM-12:20 PM	**S21A-2162. An Earthquake Rupture Forecast Inversion Applied to Fault Systems in California** M.T. Page; E.H. Field; K. Milner
8:00-8:00 AM	**S21A-2162. An Earthquake Rupture Forecast Inversion Applied to Fault Systems in California** M.T. Page; E.H. Field; K. Milner
8:00 AM-12:20 PM, Halls A-C (Moscone South), **S21B. The Future of Structural Seismology IV Posters**	
8:00 AM-12:20 PM	**S21B-2197. Modeling Broadband motions from the Tohoku earthquake** D. Li; R. Chu; R.W. Graves; D.V. Helmberger; R.W. Clayton
8:00-8:00 AM	**S21B-2197. Modeling Broadband motions from the Tohoku earthquake** D. Li; R. Chu; R.W. Graves; D.V. Helmberger; R.W. Clayton
8:00-8:00 AM	**S21B-2200. SCEC UCVM – Unified California Velocity Model** P. Small; P.J. Maechling; T.H. Jordan; G.P. Ely; R. Taborda
8:00 AM-10:00 AM, Room 302 (Moscone South), **PA21A. Defining the Importance of the Geosciences I**	

8:45-9:00 AM	**PA21A-04. Operational Earthquake Forecasting and Decision-Making in a Low-Probability Environment** T.H. Jordan
8:45-9:00 AM	**PA21A-04. Operational Earthquake Forecasting and Decision-Making in a Low-Probability Environment** T.H. Jordan
8:00 AM-10:00 AM, Room 2009 (Moscone West), **S21D. The Static Versus Dynamic Earthquake Triggering Debate: What's New and What's Next? II**	
9:00-9:15 AM	**S21D-05. Coulomb stress changes imparted by simulated M>7 earthquakes to major fault surfaces in Southern California** J.C. Rollins; G.P. Ely; T.H. Jordan
10:20 AM-12:20 PM, Room 2016 (Moscone West), **T22A. Creep and Faulting in Nature, the Lab, and Theory: Mineral Reaction-Related Instabilities II**	
11:32-11:44 AM	**T22A-06. Earthquake source scaling, stress drops and radiated seismic energies of intermediate depth earthquakes** G. Prieto; G.A. Lopez; S.A. Barrett; G.C. Beroza
10:20 AM-12:20 PM, Room 2007 (Moscone West), **S22A. Progress in Understanding Intraplate Faulting III**	
11:50-12:05 PM	**S22A-07. Magnitude Uncertainty and Ground Motion Simulations of the 1811-1812 New Madrid Earthquake Sequence** L. Ramirez Guzman; R.W. Graves; K.B. Olsen; O.S. Boyd; S. Hartzell; S. Ni; P.G. Somerville; R.A. Williams; J. Zhong
11:50-12:05 PM	**S22A-07. Magnitude Uncertainty and Ground Motion Simulations of the 1811-1812 New Madrid Earthquake Sequence** L. Ramirez Guzman; R.W. Graves; K.B. Olsen; O.S. Boyd; S. Hartzell; S. Ni; P.G. Somerville; R.A. Williams; J. Zhong
1:40 PM-6:00 PM, Halls A-C (Moscone South), **IN23B. Software Reuse and Open Source Software in Earth Science II Posters**	
1:40 PM-6:00 PM	**IN23B-1448. SCEC Broadband Platform Strong Ground Motion Simulations** S. Kumar; S. Callaghan; P.J. Maechling; K.B. Olsen; R.J. Archuleta; P.G. Somerville; R.W. Graves; T.H. Jordan
1:40-1:40 PM	**IN23B-1451. New developments and applicability of the Collaboratory for the Study of Earthquake Predictability (CSEP) testing framework** M. Liukis; D. Schorlemmer; J. Yu; P.J. Maechling; J.D. Zechar; T.H. Jordan
1:40 PM-6:00 PM, Halls A-C (Moscone South), **S23B. Observations and Modeling of Tremor and Slow Slip and Implications for Plate Boundaries I Posters**	
1:40 PM-6:00 PM	**S23B-2271. Search for Non-Volcanic Tremor in the Aftermath of the 2010 M8.8 Maule, Chile Earthquake** R.J. Walters; G.C. Beroza; S. Ide
1:40-1:40 PM	**S23B-2271. Search for Non-Volcanic Tremor in the Aftermath of the 2010 M8.8 Maule, Chile Earthquake** R.J. Walters; G.C. Beroza; S. Ide

1:40-1:40 PM	**S23B-2276. Auto-correlation Clustering Event Detection Applied to Tectonic Tremor** A.C. Aguiar; G.C. Beroza
1:40 PM-3:40 PM, Room 103 (Moscone South), **U23C. Predicting Extreme Events in Natural and Socioeconomic Systems: State-of-the-Art and Emerging Possibilities II (Video On-Demand)**	
2:40-2:55 PM	**U23C-05. Tracking Earthquake Cascades *(Invited)*** T.H. Jordan

Wednesday, December 07, 2011

Time	Session Info
8:00 AM-12:20 PM, Halls A-C (Moscone South), **S31A. Earthquake Statistics I Posters**	
8:00 AM-12:20 PM	**S31A-2214. Application of Second-Moment Source Analysis to Three Problems in Earthquake Forecasting** J. Donovan; T.H. Jordan
8:00 AM-10:00 AM, Room 2007 (Moscone West), **S31G. Observations and Modeling of Tremor and Slow Slip and Implications for Plate Boundaries II**	
9:00-9:15 AM	**S31G-05. Discriminating Tectonic Tremor from Magmatic Processes in Observationally Challenging Environments** J.R. Brown; G.C. Beroza

Thursday, December 08, 2011

Time	Session Info
8:00 AM-10:00 AM, Room 104 (Moscone South), **U41D. The Great 11 March 2011 Tohoku Earthquake III (Video On-Demand)**	
9:44-10:00 AM	**U41D-07. Shaking and flooding by the Tohoku-Oki Earthquake** S. Wei; D.V. Helmberger; R.W. Graves; H. Kanamori; J. Avouac
10:20 AM-12:20 PM, Room 2012 (Moscone West), **T42A. Grain to Basin Scale Numerical Modeling of Deformation I**	
11:35-11:50 AM	**T42A-06. A Discrete Element Modeling Approach to Exploring the Transition Between Fault-related Folding Styles** A.N. Hughes; N.P. Benesh; R.C. Alt II; J.H. Shaw
11:35-11:50 AM	**T42A-06. A Discrete Element Modeling Approach to Exploring the Transition Between Fault-related Folding Styles** A.N. Hughes; N.P. Benesh; R.C. Alt II; J.H. Shaw
1:40 PM-6:00 PM, Halls A-C (Moscone South), **S43C. Toward Seismic Rupture Models with Constraints from Experimental and Seismological Observations I Posters**	

1:40 PM-6:00 PM	**S43C-2258. Rupture behavior and ground motion from 3D simulations of the Casa Loma – Claremont stepover on the San Jacinto Fault, southern California** J. Lozos; D.D. Oglesby; J.N. Brune; K.B. Olsen
1:40-1:40 PM	**S43C-2258. Rupture behavior and ground motion from 3D simulations of the Casa Loma – Claremont stepover on the San Jacinto Fault, southern California** J. Lozos; D.D. Oglesby; J.N. Brune; K.B. Olsen

Friday, December 09, 2011

Time	Session Info
8:00 AM-12:20 PM, Halls A-C (Moscone South), **U51B. The Great 11 March 2011 Tohoku Earthquake V Posters**	
8:00 AM-12:20 PM	**U51B-0032. Shallow Dynamic Overshoot and Energetic Deep Rupture in the 2011 Mw 9.0 Tohoku-Oki Earthquake** S. Ide; A. Baltay; S. Tamura; G.C. Beroza
8:00 AM-12:20 PM, Halls A-C (Moscone South), **NH51B. Observations, Modeling, and Economics of Extreme Events I Posters**	
8:00 AM-12:20 PM	**NH51B-1696. Broadband CyberShake Platform: Seismogram Synthesis for Broadband Physics-Based Probabilistic Seismic Hazard Analysis** S. Callaghan; P.J. Maechling; P. Small; K. Milner; R.W. Graves; T.H. Jordan
8:00 AM-12:20 PM, Halls A-C (Moscone South), **DI51A. Earth's Heterogeneous Mantle I Posters**	
8:00 AM-12:20 PM	**DI51A-2119. Global Correlations of Mantle Structure with Crustal Tectonic Regions** E. Paulson; T.H. Jordan
8:00 AM-12:20 PM, Halls A-C (Moscone South), **S51B. Numerical Seismology I Posters**	
8:00 AM-12:20 PM	**S51B-2214. Directivity-Basin Coupling in the Los Angeles Region from the CyberShake Hazard Model** F. Wang; T.H. Jordan; S. Callaghan; K. Milner; P.J. Maechling; R.W. Graves
8:00-8:00 AM	**S51B-2215. A Unified Finite Element Method for Arbitrary Elastic and Acoustic Media** H. Karaoglu; J. Bielak
8:00-8:00 AM	**S51B-2215. A Unified Finite Element Method for Arbitrary Elastic and Acoustic Media** H. Karaoglu; J. Bielak
8:00 AM-12:20 PM, Halls A-C (Moscone South), **S51C. Structure I Posters**	

8:00 AM-12:20 PM	**S51C-2244. Station-to-Station Green's Functions Extracted From Seismic Coda in Southern California** E.T. Hirakawa; S. Ma
8:00-8:00 AM	**S51C-2244. Station-to-Station Green's Functions Extracted From Seismic Coda in Southern California** E.T. Hirakawa; S. Ma
8:00 AM-12:20 PM, Halls A-C (Moscone South), **T51C. Grain to Basin Scale Numerical Modeling of Deformation II Posters**	
8:00 AM-12:20 PM	**T51C-2347. Incorporating fault-slip constraints in 3D geomechanical restoration with application to restraining bend systems in the deep-water Niger Delta.** P. Durand-Riard; J.H. Shaw; A. Plesch
8:00-8:00 AM	**T51C-2347. Incorporating fault-slip constraints in 3D geomechanical restoration with application to restraining bend systems in the deep-water Niger Delta.** P. Durand-Riard; J.H. Shaw; A. Plesch
8:00 AM-10:00 AM, Room 3024 (Moscone West), **S51E. Big Sources**	
8:15-8:30 AM	**S51E-02. Radiated Energy of Great Earthquakes** A. Baltay; S. Ide; G.C. Beroza
8:15-8:30 AM	**S51E-02. Radiated Energy of Great Earthquakes** A. Baltay; S. Ide; G.C. Beroza
8:00 AM-10:00 AM, Room 2009 (Moscone West), **S51D. 3D Seismic Imaging IV**	
9:00-9:15 AM (Conflict)	**S51D-05. Full-3D Waveform Tomography for Southern California** E. Lee; P. Chen; T.H. Jordan; P.J. Maechling; M. Denolle; G.C. Beroza
8:00 AM-10:00 AM, Room 3024 (Moscone West), **S51E. Big Sources**	
9:00-9:15 AM (Conflict)	**S51E-05. Ground Motion Prediction for a scenario M 7 Earthquake on the Southern San Andreas Fault Using the Virtual Source Approach** M. Denolle; E.M. Dunham; G.C. Beroza; G. Prieto
10:20 AM-12:20 PM, Rooms 2022-2024 (Moscone West), **S52A. Earthquake Early Warning Capabilities and Delivery Around the World II (Video On-Demand)**	
10:20-10:35 AM	**S52A-01. CISN ShakeAlert: Delivering test warnings for California earthquakes** R.M. Allen; M. Boese; H. Brown; M. Caprio; G.B. Cua; M. Fischer; D.D. Given; E. Hauksson; T.H. Heaton; M. Hellweg; I. Henson; M. Liukis; P.J. Maechling; M.A. Meier; D.S. Neuhauser; D.H. Oppenheimer; K. Solanki
11:35-11:50 AM (Conflict)	**S52A-07. Near Real-time Full-wave Centroid Moment Tensor (CMT) Inversion for Ground-motion forecast in 3D Earth Structure of Southern California** P. Chen; E. Lee; T.H. Jordan; P.J. Maechling
10:20 AM-12:20 PM, Room 2005 (Moscone West), **S52B. Toward Seismic Rupture Models with Constraints from Experimental and Seismological Observations II**	

11:35-11:50 AM (Conflict)	**S52B-06. Broadband Ground Motion Simulations for a Kinematic Variation of the Mw 7.8 ShakeOut Rupture** R.W. Graves; E. Seyhan; J.P. Stewart
1:40 PM-6:00 PM, Halls A-C (Moscone South), **S53A. Earthquake Early Warning Capabilities and Delivery Around the World III Posters**	
1:40 PM-6:00 PM	**S53A-2255. Development of ShakeAlert Performance Evaluation Software** P.J. Maechling; M. Liukis; T.H. Jordan
1:40 PM-3:40 PM, Room 2011 (Moscone West), **T53C. Earthquake Geology and Seismotectonics in South and East Asia III**	
2:25-2:40 PM	**T53C-04. Active blind-thrust faulting and growth folding in the southern Longmen Shan, eastern Tibetan Plateau** M. Wang; D. Jia; J.H. Shaw; A. Lin; B. Liu; Y. Li
4:00 PM-6:00 PM, Room 2005 (Moscone West), **S54C. Toward Seismic Rupture Models with Constraints from Experimental and Seismological Observations IV**	
5:30-5:45 PM	**S54C-07. Effect of Sediments on Rupture Dynamics of Shallow Subduction Zone Earthquakes and Tsunami Generation** S. Ma

Final ID: T11A-2274

Strain localization and crustal thickness variation across major strike slip faults in southern California revealed by receiver function studies

P. Zhang; [1]; *M. S. Miller;* [1]; *J. F. Dolan;* [1]; *I. W. Bailey;* [1]; *D. A. Okaya;* [1];
1. Earth Sciences, USC, Los Angeles, CA, United States.

Body: The degree to which faults are localized or distributed within the continental lithosphere has been a controversial subject for decades. Reflection and refraction studies indicate that the San Andreas fault (SAF) extends into the lower crust as a narrow fault zone in northern California and along the Mojave segment of the fault. However, the discreteness of lithospheric deformation along the southernmost segments of the SAF system (e.g., the Elsinore, the San Jacinto and the Coachella segment of the San Andreas) remains unclear. We have begun a detailed study of how the distribution of strain at depth is in southern California using P receiver functions to image crustal and lithospheric thickness variations. We specifically focus on the depths of the Moho and lithosphere-asthenosphere boundary (LAB) underneath the major faults. Our results for the geometry of crustal and lithospheric interfaces provide insight into the strain localization in this region. Our preliminary results using events recorded by Southern California Seismic Network and USarray reveal complex crustal and lithospheric structure in this region. A SW-NE profile across the Elsinore, San Jacinto, and and San Andreas faults indicates that the Moho dips to the southwest. Moreover, receiver gathers at certain stations near the faults show a strong back-azimuthal variation. Using simple velocity models to project the Ps conversions to depth, we find that some of the back-azimuth variation can be related to different sides of the faults. These back-azimuthal variations of the Moho signal indicate three-dimensional complexity beneath the central San Jacinto fault that may suggest strain localization at these depths. We assess the robustness of these features with respect to the choice of velocity model and method resolution using synthetic waveform modeling.

Final ID: T11A-2279

Characterizing the recent behavior and earthquake potential of the blind western San Cayetano and Ventura fault systems

L. J. McAuliffe; [1]; *J. F. Dolan;* [1]; *J. Hubbard;* [2]; *J. H. Shaw;* [2];

1. Dept. of Earth Sciences, University of Southern California, Los Angeles, CA, United States.
2. Dept. of Earth & Planetary Sciences, Harvard University, Cambridge, MA, United States.

Body: The recent occurrence of several destructive thrust fault earthquakes highlights the risks posed by such events to major urban centers around the world. In order to determine the earthquake potential of such faults in the western Transverse Ranges of southern California, we are studying the activity and paleoearthquake history of the blind Ventura and western San Cayetano faults through a multidisciplinary analysis of strata that have been folded above the fault tiplines. These two thrust faults form the middle section of a >200-km-long, east-west belt of large, interconnected reverse faults that extends across southern California. Although each of these faults represents a major seismic source in its own right, we are exploring the possibility of even larger-magnitude, multi-segment ruptures that may link these faults to other major faults to the east and west in the Transverse Ranges system. The proximity of this large reverse-fault system to several major population centers, including the metropolitan Los Angeles region, and the potential for tsunami generation during offshore ruptures of the western parts of the system, emphasizes the importance of understanding the behavior of these faults for seismic hazard assessment.

During the summer of 2010 we used a mini-vibrator source to acquire four, one- to three-km-long, high-resolution seismic reflection profiles. The profiles were collected along the locus of active folding above the blind, western San Cayetano and Ventura faults - specifically, across prominent fold scarps that have developed in response to recent slip on the underlying thrust ramps. These high-resolution data overlap with the uppermost parts of petroleum-industry seismic reflection data, and provide a near-continuous image of recent folding from several km depth to within 50-100 m of the surface.

Our initial efforts to document the earthquake history and slip-rate of this large, multi-fault reverse fault system focus on a site above the blind, western San Cayetano thrust ramp. At Briggs Road ~14 km east of Ventura, a high-resolution profile across the locus of recent folding reveals a well-defined north-dipping active synclinal axial surface in growth strata that extends to the surface at a prominent south-facing fold scarp lying at the topographic range front. During August 2011, we drilled 11 hollow-stem boreholes and cone-penetrometer tests along the same alignment as the reflection profile, providing overlap between the data sets. Preliminary analysis of the borehole data reveals a fine-grained section dominated by thinly bedded silts and sands. The absence of any well-developed soils within the upper 20 m, coupled with at least 15 m of structural growth within this section, suggests a rapid slip rate that we will quantify with radiocarbon dating of detrital charcoal and several buried organic-rich A horizons. Collectively, we anticipate that these borehole and high-resolution seismic reflection data will yield a detailed record of the fold growth during recent large earthquakes at this site, which will in turn allow us to reconstruct the paleoseismic history of the underlying blind thrust ramp.

Final ID: IN11D-02

A Parallel Simulated Annealing Approach to Solve for Earthquake Rupture Rates

K. Milner; [1]; *M. T. Page;* [2]; *E. H. Field;* [3];

1. Earth Sciences, Univ of Southern California, Los Angeles, CA, United States.
2. United States Geological Survey, Pasadena, CA, United States.
3. United States Geological Survey, Golden, CO, United States.

Body: We present a parallel approach to the classic simulated annealing algorithm (Kirkpatrick 1983) in order to solve for the rates of earthquake ruptures in California's complex fault system, being developed for the 3rd Uniform California Earthquake Rupture Forecast (UCERF3). Through the use of distributed computing, we have achieved substantial speedup when compared to serial simulated annealing. We will describe the parallel simulated annealing algorithm in detail, as well as the parallelization parameters used and their effect on speedup (time to convergence, or alternatively a specified energy level) and communications efficiency. Additionally we will discuss the correlation between performance of the parallel algorithm and the degree of constraints on the solution. We will present scaling results to thousands of processors, and experiences with the MPJ Express Java Message Passing Library (Baker 2006) on the University of Southern California's High Performance Computing and Communications cluster.

References:

Mark Baker, Bryan Carpenter, and Aamir Shafi. MPJ Express: Towards Thread Safe Java HPC, Submitted to the IEEE International Conference on Cluster Computing (Cluster 2006), Barcelona, Spain, 25-28 September, 2006.

S. Kirkpatrick, C. D. Gelatt, Jr., and M. P. Vecchi. Optimization by Simulated Annealing. Science 13 May 1983: 220 (4598), 671-680. [DOI:10.1126/science.220.4598.671]

Final ID: S11D-03

Seismological Constraints on the Deep Structure of Continents *(Invited)*

T. H. Jordan; [1]; *E. Paulson;* [1];

1. Dept of Earth Sciences ZHS-169, Univ of Southern California, Los Angeles, CA, United States.

Body: While it is generally agreed that the cratons are underlain by thick, basalt-depleted keels in near-isopycnic balance, the maximum thickness of the keels has remained controversial since this theory of the continental tectosphere was proposed in the mid-1970s. Recent reviews have combined tomographic models with other information to conclude that cratonic keels achieve maximum depths of 200-250 km. Here we show that this inference is not consistent with some first-order aspects of upper-mantle tomography. In a meta-analysis of more than 20 whole-mantle tomographic models published by various research groups, we estimate the correlation between upper-mantle seismic structure and crustal tectonic structure by projecting the tomographic models onto the GTR1 global tectonic regionalization. These projections show consistent and statistically significant cratonic signatures extending to depths exceeding 300 km. In particular, the average shear velocities of stable continental regions in the depth interval 200-400 km are higher than those of the convecting oceanic mantle, and the corresponding shear-velocity gradients are significantly lower, in good agreement with high-resolution regional models derived from multi-phase waveform inversions. We conclude that the average thickness of the cratonic tectosphere is unlikely to be less than 300 km; indeed, beneath some (if not most) cratons, the keels nearly fill the entire upper mantle. The isopycnic requirements for thick cratonic tectosphere place strong constraints on models of continental formation and evolution.

Final ID: G13A-0872

Rapid Determination of Near-Fault Earthquake Deformation Using LIDAR

A. A. Borsa; [1, 2]; *J. H. Minster;* [2];

1. UNAVCO, Boulder, CO, United States.
2. UC San Diego, La Jolla, CA, United States.

Body: The 2005 airborne lidar survey of the southern San Andreas, San Jacinto and Banning faults (the “B4 Survey”) has delivered a high-resolution digital elevation model (DEM) of 1100 km of the most seismically active fault systems in southern California for the express purpose of providing a baseline for post-earthquake slip determination. We used this survey as a testbed to experiment with processing algorithms for rapid estimation of near-fault ground deformation. One algorithm uses simultaneous cross correlation of both topography and backscatter intensity from pre-earthquake and simulated post-earthquake LIDAR datasets. We show robust recovery of the direction and magnitude of an applied synthetic slip of 5 m in the horizontal and 0.5 m in the vertical within the test area, with excellent discrimination between areas with and without applied slip. Another algorithm relies on an evolutionary programming approach, which is more robust in the presence of multiple minima of the solution manifold, but requires substantially more processing power. Our results indicate that one should be able to recover slip to accuracies of better than 20 cm in the horizontal and 1 cm in the vertical, at a spatial resolution of ≤15 m for lidar datasets with sample densities as low as 0.5 points/m2.

Final ID: IN13A-1318

Acceleration of 3D Finite Difference AWP-ODC for seismic simulation on GPU Fermi Architecture

J. Zhou; [1]; *Y. Cui;* [1]; *D. Choi;* [1];

1. San Diego Supercopmuter Center, La Jolla, CA, United States.

Body: AWP-ODC, a highly scalable parallel finite-difference application, enables petascale 3D earthquake calculations. This application generates realistic dynamic earthquake source description and detailed physics-based anelastic ground motions at frequencies pertinent to safe building design. In 2010, the code achieved M8, a full dynamical simulation of a magnitude-8 earthquake on the southern San Andreas fault up to 2-Hz, the largest-ever earthquake simulation.

Building on the success of the previous work, we have implemented CUDA on AWP-ODC to accelerate wave propagation on GPU platform. Our CUDA development aims on aggressive parallel efficiency, optimized global and shared memory access to make the best use of GPU memory hierarchy. The benchmark on NVIDIA Tesla C2050 graphics cards demonstrated many tens of speedup in single precision compared to serial implementation at a testing problem size, while an MPI-CUDA implementation is in the progress to extend our solver to multi-GPU clusters. Our CUDA implementation has been carefully verified for accuracy.

Final ID: T13A-2350

Detection of repeating and "anti-repeating" earthquakes in the Bucaramanga Nest

S. A. Barrett; [1]; *G. Prieto;* [2]; *G. C. Beroza;* [1];

1. Geophysics, Stanford University, Stanford, CA, United States.
2. Departamento de Física, Universidad de los Andes, Bogota, Colombia.

Body: The Bucaramanga Nest, beneath northern Colombia represents the densest concentration of intermediate-depth earthquakes in the world. The roughly 11 km3 volume produces approximately 15 events per day, yielding an active catalog of seismicity well separated from surrounding seismic activity. We correlate template-event waveforms from known earthquakes to continuous records from the Colombian National (RSNC) seismic network. Typical repeating events are identified as well as the more curious “anti-repeat” events for which seismograms show reversed polarity and nearly perfect anti-correlation. These events are of particular interest as they are not known for shallow, crustal earthquake populations. By compiling a more complete catalog of earthquakes, and by developing precise relative locations, we seek to understand the temporal and size variations of these recurring events in the Bucaramanga Nest.

Final ID: T13G-05

Structure and seismic hazard of the Ventura Avenue anticline and Ventura fault, California

J. Hubbard; [1]; *J. H. Shaw;* [1]; *J. F. Dolan;* [2]; *T. L. Pratt;* [3, 4]; *L. J. McAuliffe;* [2];

1. Earth & Planet. Sci., Harvard Univ., Cambridge, MA, United States.
2. Earth Sci., USC, Los Angeles, CA, United States.
3. Earth & Space Sci., Univ. of Wash., Seattle, WA, United States.
4. USGS, Seattle, WA, United States.

Body: The Ventura Avenue anticline, in the western Transverse Ranges, is one of the fastest uplifting structures in southern California, rising at a rate of ~5 mm/yr (Rockwell et al., 1988). However, there is disagreement about whether this structure poses a seismic hazard, due to uncertainty about the nature of the Ventura fault, which lies along the southern margin of the fold. Two models have been proposed: either the Ventura fault extends to seismogenic depths beneath the anticline (e.g., Sarna-Wojcicki et al., 1976), or it is a shallow, bending-moment fault that does not pose a significant seismic hazard (e.g., Yeats, 1982a,b; Huftile and Yeats, 1995). Seismic data across the tip of the Ventura fault suggest that it deforms late Pleistocene and younger strata, implying that the fault system is active. Given that the fault trace extends directly through the city of Ventura, distinguishing between these two interpretations has considerable importance in regional seismic hazard assessments.

We use well data, industry seismic reflection profiles, and two seismic profiles acquired by our group in August 2010, to construct a more complete 3D model of the system. Based on dipmeter logs and stratigraphic cutoffs imaged in seismic reflection profiles, we show that the north-dipping Ventura fault extends to seismogenic depth beneath the anticline. Fault offset increases with depth, implying that the Ventura fault has propagated upwards over time. Thus, we interpret the Ventura Avenue anticline to be a fault-propagation fold underlain by an active thrust ramp. A decrease in the uplift rate of the anticline at 30 ka, as measured from uplifted terraces (Rockwell et al., 1988), is consistent with a breakthrough of the Ventura fault at that time, although the fault is still blind as it is buried by a sedimentary cover.

In order to assess the hazard of the fault, we examine its regional extent. The Ventura fold trend continues offshore and coincides with a set of oil fields. A 3D seismic dataset across the Dos Cuadras field, which lies along the trend, shows that it is a fault-propagation fold, structurally similar to the Ventura Avenue anticline. Dos Cuadras is also underlain by a north-dipping thrust fault, known as the Pitas Point thrust. Based on our and others' mapping, the Ventura and Pitas Point faults form an en echelon system that extends at least 40 km offshore. Other regional faults, including the San Cayetano, Lion, and Red Mountain faults, link with the Ventura/Pitas Point system at depth; we suggest that at 15 km depth, these faults may all link into a single, continuous fault surface.

One of the greatest hazards in fold-and-thrust belts is the risk of large, multi-segment ruptures. Linkage of the Ventura/Pitas Point fault could generate a M7.3 earthquake, while rupture in association with other regional faults could produce even larger events. We provide 3D models of these faults and estimate the magnitudes of potential multi-segment earthquakes. Finally, we show that GPS data are consistent with a very high shortening rate (> 6 mm/yr) across the anticline, reinforcing the hazardous nature of the system.

Final ID: T13G-05

Structure and seismic hazard of the Ventura Avenue anticline and Ventura fault, California

J. Hubbard; [1]; *J. H. Shaw;* [1]; *J. F. Dolan;* [2]; *T. L. Pratt;* [3, 4]; *L. J. McAuliffe;* [2];

1. Earth & Planet. Sci., Harvard Univ., Cambridge, MA, United States.
2. Earth Sci., USC, Los Angeles, CA, United States.
3. Earth & Space Sci., Univ. of Wash., Seattle, WA, United States.
4. USGS, Seattle, WA, United States.

Body: The Ventura Avenue anticline, in the western Transverse Ranges, is one of the fastest uplifting structures in southern California, rising at a rate of ~5 mm/yr (Rockwell et al., 1988). However, there is disagreement about whether this structure poses a seismic hazard, due to uncertainty about the nature of the Ventura fault, which lies along the southern margin of the fold. Two models have been proposed: either the Ventura fault extends to seismogenic depths beneath the anticline (e.g., Sarna-Wojcicki et al., 1976), or it is a shallow, bending-moment fault that does not pose a significant seismic hazard (e.g., Yeats, 1982a,b; Huftile and Yeats, 1995). Seismic data across the tip of the Ventura fault suggest that it deforms late Pleistocene and younger strata, implying that the fault system is active. Given that the fault trace extends directly through the city of Ventura, distinguishing between these two interpretations has considerable importance in regional seismic hazard assessments.

We use well data, industry seismic reflection profiles, and two seismic profiles acquired by our group in August 2010, to construct a more complete 3D model of the system. Based on dipmeter logs and stratigraphic cutoffs imaged in seismic reflection profiles, we show that the north-dipping Ventura fault extends to seismogenic depth beneath the anticline. Fault offset increases with depth, implying that the Ventura fault has propagated upwards over time. Thus, we interpret the Ventura Avenue anticline to be a fault-propagation fold underlain by an active thrust ramp. A decrease in the uplift rate of the anticline at 30 ka, as measured from uplifted terraces (Rockwell et al., 1988), is consistent with a breakthrough of the Ventura fault at that time, although the fault is still blind as it is buried by a sedimentary cover.

In order to assess the hazard of the fault, we examine its regional extent. The Ventura fold trend continues offshore and coincides with a set of oil fields. A 3D seismic dataset across the Dos Cuadras field, which lies along the trend, shows that it is a fault-propagation fold, structurally similar to the Ventura Avenue anticline. Dos Cuadras is also underlain by a north-dipping thrust fault, known as the Pitas Point thrust. Based on our and others' mapping, the Ventura and Pitas Point faults form an en echelon system that extends at least 40 km offshore. Other regional faults, including the San Cayetano, Lion, and Red Mountain faults, link with the Ventura/Pitas Point system at depth; we suggest that at 15 km depth, these faults may all link into a single, continuous fault surface.

One of the greatest hazards in fold-and-thrust belts is the risk of large, multi-segment ruptures. Linkage of the Ventura/Pitas Point fault could generate a M7.3 earthquake, while rupture in association with other regional faults could produce even larger events. We provide 3D models of these faults and estimate the magnitudes of potential multi-segment earthquakes. Finally, we show that GPS data are consistent with a very high shortening rate (> 6 mm/yr) across the anticline, reinforcing the hazardous nature of the system.

Final ID: DI14A-08

PyLith: A Finite-Element Code for Modeling Quasi-Static and Dynamic Crustal Deformation *(Invited)*

B. Aagaard; [1]; *C. A. Williams;* [2]; *M. G. Knepley;* [3];

1. USGS MS977, Menlo Park, CA, United States.
2. GNS Science, Lower Hutt, New Zealand.
3. Computation Institute, University of Chicago, Chicago, IL, United States.

Body: We have developed open-source finite-element software for 2-D and 3-D dynamic and quasi-static modeling of crustal deformation. This software, PyLith (current release is version 1.6) can be used for quasi-static viscoelastic modeling, dynamic spontaneous rupture and/or ground-motion modeling. Unstructured and structured finite-element discretizations allow for spatial scales ranging from tens of meters to hundreds of kilometers with temporal scales in dynamic problems ranging from milliseconds to minutes and temporal scales in quasi-static problems ranging from minutes to thousands of years. PyLith development is part of the NSF funded Computational Infrastructure for Geodynamics (CIG) and the software runs on a wide variety of platforms (laptops, workstations, and Beowulf clusters). Binaries (Linux, Darwin, and Windows systems) and source code are available from geodynamics.org. PyLith uses a suite of general, parallel, graph data structures called Sieve for storing and manipulating finite-element meshes. This permits use of a variety of 2-D and 3-D cell types including triangles, quadrilaterals, hexahedra, and tetrahedra.

Current PyLith features include prescribed fault ruptures with multiple earthquakes and aseismic creep, spontaneous fault ruptures with a variety of fault constitutive models, time-dependent Dirichlet and Neumann boundary conditions, absorbing boundary conditions, time-dependent point forces, and gravitational body forces. PyLith supports infinitesimal and small strain formulations for linear elastic rheologies, linear and generalized Maxwell viscoelastic rheologies, power-law viscoelastic rheologies, and Drucker-Prager elastoplastic rheologies. Current software development focuses on coupling quasi-static and dynamic simulations to resolve multi-scale deformation across the entire seismic cycle and the coupling of elasticity to heat and/or fluid flow.

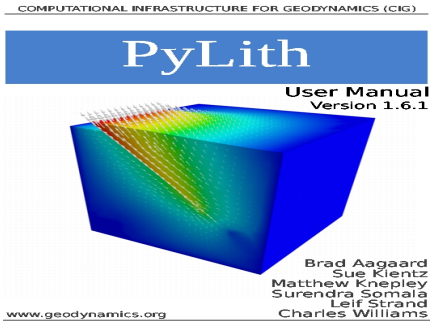

Final ID: DI14A-08

PyLith: A Finite-Element Code for Modeling Quasi-Static and Dynamic Crustal Deformation *(Invited)*

B. Aagaard; [1]; *C. A. Williams;* [2]; *M. G. Knepley;* [3];

1. USGS MS977, Menlo Park, CA, United States.
2. GNS Science, Lower Hutt, New Zealand.
3. Computation Institute, University of Chicago, Chicago, IL, United States.

Body: We have developed open-source finite-element software for 2-D and 3-D dynamic and quasi-static modeling of crustal deformation. This software, PyLith (current release is version 1.6) can be used for quasi-static viscoelastic modeling, dynamic spontaneous rupture and/or ground-motion modeling. Unstructured and structured finite-element discretizations allow for spatial scales ranging from tens of meters to hundreds of kilometers with temporal scales in dynamic problems ranging from milliseconds to minutes and temporal scales in quasi-static problems ranging from minutes to thousands of years. PyLith development is part of the NSF funded Computational Infrastructure for Geodynamics (CIG) and the software runs on a wide variety of platforms (laptops, workstations, and Beowulf clusters). Binaries (Linux, Darwin, and Windows systems) and source code are available from geodynamics.org. PyLith uses a suite of general, parallel, graph data structures called Sieve for storing and manipulating finite-element meshes. This permits use of a variety of 2-D and 3-D cell types including triangles, quadrilaterals, hexahedra, and tetrahedra.

Current PyLith features include prescribed fault ruptures with multiple earthquakes and aseismic creep, spontaneous fault ruptures with a variety of fault constitutive models, time-dependent Dirichlet and Neumann boundary conditions, absorbing boundary conditions, time-dependent point forces, and gravitational body forces. PyLith supports infinitesimal and small strain formulations for linear elastic rheologies, linear and generalized Maxwell viscoelastic rheologies, power-law viscoelastic rheologies, and Drucker-Prager elastoplastic rheologies. Current software development focuses on coupling quasi-static and dynamic simulations to resolve multi-scale deformation across the entire seismic cycle and the coupling of elasticity to heat and/or fluid flow.

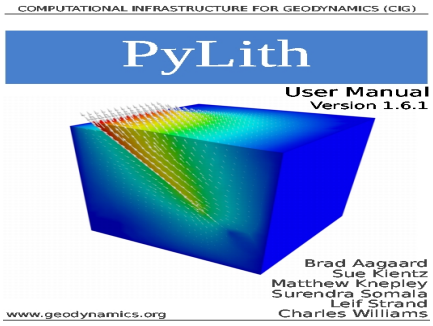

Final ID: S21A-2162

An Earthquake Rupture Forecast Inversion Applied to Fault Systems in California

M. T. Page; [1]; *E. H. Field;* [2]; *K. Milner;* [3];

1. USGS, Pasadena, CA, United States.
2. USGS, Golden, CO, United States.
3. USC, Los Angeles, CA, United States.

Body: Previous fault-based rupture forecasts for California have been plagued with magnitude “bulges” and fail to simultaneously fit all available data. We present results from an inversion-based methodology being developed for the 3rd Uniform California Earthquake Rupture Forecast (UCERF3) that simultaneously satisfies available slip-rate, paleoseismic event-rate, and magnitude-distribution constraints. Using a parallel simulated-annealing algorithm, we solve for the rates of all ruptures that extend through the seismogenic thickness on major mapped faults in California. This inverse approach eliminates the need for expert-opinion voting on rupture rates themselves, allowing for more transparent and reproducible results than previous earthquake rupture forecasts. The inversion methodology also allows for the incorporation of multi-fault ruptures, which eliminates the magnitude-distribution misfits that were present in earlier models. Furthermore, we show that the inversion solutions match slip-rate and paleoseismic event-rate data better than previous models.

Final ID: S21A-2162

An Earthquake Rupture Forecast Inversion Applied to Fault Systems in California

M. T. Page; [1]; *E. H. Field;* [2]; *K. Milner;* [3];

1. USGS, Pasadena, CA, United States.
2. USGS, Golden, CO, United States.
3. USC, Los Angeles, CA, United States.

Body: Previous fault-based rupture forecasts for California have been plagued with magnitude “bulges” and fail to simultaneously fit all available data. We present results from an inversion-based methodology being developed for the 3rd Uniform California Earthquake Rupture Forecast (UCERF3) that simultaneously satisfies available slip-rate, paleoseismic event-rate, and magnitude-distribution constraints. Using a parallel simulated-annealing algorithm, we solve for the rates of all ruptures that extend through the seismogenic thickness on major mapped faults in California. This inverse approach eliminates the need for expert-opinion voting on rupture rates themselves, allowing for more transparent and reproducible results than previous earthquake rupture forecasts. The inversion methodology also allows for the incorporation of multi-fault ruptures, which eliminates the magnitude-distribution misfits that were present in earlier models. Furthermore, we show that the inversion solutions match slip-rate and paleoseismic event-rate data better than previous models.

Final ID: S21B-2197

Modeling Broadband motions from the Tohoku earthquake

D. Li; [1]; *R. Chu;* [1]; *R. W. Graves;* [2]; *D. V. Helmberger;* [1]; *R. W. Clayton;* [1];

1. Caltech, Pasadena, CA, United States.
2. US Geological Survey , Pasadena, CA, United States.

Body: The 2011 M9 Tohoku earthquake produced an extraordinary dataset of over 2000 broadband regional and teleseismic records. While considerable progress has been made in modeling the longer period (>3 s) waveforms, the shorter periods (1-3 s) prove more difficult. Since modeling high frequency waveforms in 3D is computationally expensive, we follow the approach proposed by Helmberger and Vidale (1988), which interfaces the Cagniard-de Hoop analytical source description with a 2D numerical code to account for earthquake radiation patterns. We extend this method to a staggered grid finite difference code, which is stable in the presence of water. The code adapts the Convolutional PML boundary condition, and uses the “following the wavefront” technique and multiple GPUs, which significantly reduces computing time. We test our method against existing 1D and 3D codes, and examine the effects of slab structure, ocean bathymetry and local basins in an attempt to better explain the observed shorter period response.

Final ID: S21B-2197

Modeling Broadband motions from the Tohoku earthquake

D. Li; [1]; *R. Chu;* [1]; *R. W. Graves;* [2]; *D. V. Helmberger;* [1]; *R. W. Clayton;* [1];

1. Caltech, Pasadena, CA, United States.
2. US Geological Survey , Pasadena, CA, United States.

Body: The 2011 M9 Tohoku earthquake produced an extraordinary dataset of over 2000 broadband regional and teleseismic records. While considerable progress has been made in modeling the longer period (>3 s) waveforms, the shorter periods (1-3 s) prove more difficult. Since modeling high frequency waveforms in 3D is computationally expensive, we follow the approach proposed by Helmberger and Vidale (1988), which interfaces the Cagniard-de Hoop analytical source description with a 2D numerical code to account for earthquake radiation patterns. We extend this method to a staggered grid finite difference code, which is stable in the presence of water. The code adapts the Convolutional PML boundary condition, and uses the “following the wavefront” technique and multiple GPUs, which significantly reduces computing time. We test our method against existing 1D and 3D codes, and examine the effects of slab structure, ocean bathymetry and local basins in an attempt to better explain the observed shorter period response.

Final ID: S21B-2200

SCEC UCVM – Unified California Velocity Model

P. Small; [1]; *P. J. Maechling;* [1]; *T. H. Jordan;* [1]; *G. P. Ely;* [2, 1]; *R. Taborda;* [3];

1. University of Southern California, Los Angeles, CA, United States.
2. Argonne National Laboratory, Argonne, IL, United States.
3. Carnegie Mellon University, Pittsburg, PA, United States.

Body: The SCEC Unified California Velocity Model (UCVM) is a software framework for a state-wide California velocity model. UCVM provides researchers with two new capabilities: (1) the ability to query Vp, Vs, and density from any standard regional California velocity model through a uniform interface, and (2) the ability to combine multiple velocity models into a single state-wide model. These features are crucial in order to support large-scale ground motion simulations and to facilitate improvements in the underlying velocity models. UCVM provides integrated support for the following standard velocity models: SCEC CVM-H, SCEC CVM-S and the CVM-SI variant, USGS Bay Area (cencalvm), Lin-Thurber Statewide, and other smaller regional models. New models may be easily incorporated as they become available. Two query interfaces are provided: a Linux command line program, and a C application programming interface (API). The C API query interface is simple, fully independent of any specific model, and MPI-friendly. Input coordinates are geographic longitude/latitude and the vertical coordinate may be either depth or elevation. Output parameters include Vp, Vs, and density along with the identity of the model from which these material properties were obtained. In addition to access to the standard models, UCVM also includes a high resolution statewide digital elevation model, Vs30 map, and an optional near-surface geo-technical layer (GTL) based on Ely's Vs30-derived GTL. The elevation and Vs30 information is bundled along with the returned Vp,Vs velocities and density, so that all relevant information is retrieved with a single query. When the GTL is enabled, it is blended with the underlying crustal velocity models along a configurable transition depth range with an interpolation function. Multiple, possibly overlapping, regional velocity models may be combined together into a single state-wide model. This is accomplished by tiling the regional models on top of one another in three dimensions in a researcher-specified order. No reconciliation is performed within overlapping model regions, although a post-processing tool is provided to perform a simple numerical smoothing. Lastly, a 3D region from a combined model may be extracted and exported into a CVM-Etree. This etree may then be queried by UCVM much like a standard velocity model but with less overhead and generally better performance due to the efficiency of the etree data structure.

URL: http://scec.usc.edu/scecpedia/UCVM

Final ID: PA21A-04

Operational Earthquake Forecasting and Decision-Making in a Low-Probability Environment

T. H. Jordan; [1];
1. Dept of Earth Sciences ZHS-169, Univ of Southern California, Los Angeles, CA, United States.

Body: Operational earthquake forecasting (OEF) is the dissemination of authoritative information about the time dependence of seismic hazards to help communities prepare for potentially destructive earthquakes. Most previous work on the public utility of OEF has anticipated that forecasts would deliver high probabilities of large earthquakes; i.e., deterministic predictions with low error rates (false alarms and failures-to-predict) would be possible. This expectation has not been realized. An alternative to deterministic prediction is probabilistic forecasting based on empirical statistical models of aftershock triggering and seismic clustering. During periods of high seismic activity, short-term earthquake forecasts can attain prospective probability gains in excess of 100 relative to long-term forecasts. The utility of such information is by no means clear, however, because even with hundredfold increases, the probabilities of large earthquakes typically remain small, rarely exceeding a few percent over forecasting intervals of days or weeks. Civil protection agencies have been understandably cautious in implementing OEF in this sort of “low-probability environment.”

The need to move more quickly has been underscored by recent seismic crises, such as the 2009 L’Aquila earthquake sequence, in which an anxious public was confused by informal and inaccurate earthquake predictions. After the L’Aquila earthquake, the Italian Department of Civil Protection appointed an International Commission on Earthquake Forecasting (ICEF), which I chaired, to recommend guidelines for OEF utilization. Our report (Ann. Geophys., 54, 4, 2011; doi: 10.4401/ag-5350) concludes: (a) Public sources of information on short-term probabilities should be authoritative, scientific, open, and timely, and need to convey epistemic uncertainties. (b) Earthquake probabilities should be based on operationally qualified, regularly updated forecasting systems. (c) All operational models should be evaluated for reliability and skill by retrospective testing, and the models should be under continuous prospective testing against long-term forecasts and alternative time-dependent models. (d) Short-term models used in operational forecasting should be consistent with the long-term forecasts used in probabilistic seismic hazard analysis. (e) Alert procedures should be standardized to facilitate decisions at different levels of government, based in part on objective analysis of costs and benefits. (f) In establishing alert protocols, consideration should also be given to the less tangible aspects of value-of-information, such as gains in psychological preparedness and resilience.

Authoritative statements of increased risk, even when the absolute probability is low, can provide a psychological benefit to the public by filling information vacuums that lead to informal predictions and misinformation. Formal OEF procedures based on probabilistic forecasting appropriately separate hazard estimation by scientists from the decision-making role of civil protection authorities. The prosecution of seven Italian scientists on manslaughter charges stemming from their actions before the L’Aquila earthquake makes clear why this separation should be explicit in defining OEF protocols.

Final ID: PA21A-04

Operational Earthquake Forecasting and Decision-Making in a Low-Probability Environment

T. H. Jordan; [1];
1. Dept of Earth Sciences ZHS-169, Univ of Southern California, Los Angeles, CA, United States.

Body: Operational earthquake forecasting (OEF) is the dissemination of authoritative information about the time dependence of seismic hazards to help communities prepare for potentially destructive earthquakes. Most previous work on the public utility of OEF has anticipated that forecasts would deliver high probabilities of large earthquakes; i.e., deterministic predictions with low error rates (false alarms and failures-to-predict) would be possible. This expectation has not been realized. An alternative to deterministic prediction is probabilistic forecasting based on empirical statistical models of aftershock triggering and seismic clustering. During periods of high seismic activity, short-term earthquake forecasts can attain prospective probability gains in excess of 100 relative to long-term forecasts. The utility of such information is by no means clear, however, because even with hundredfold increases, the probabilities of large earthquakes typically remain small, rarely exceeding a few percent over forecasting intervals of days or weeks. Civil protection agencies have been understandably cautious in implementing OEF in this sort of “low-probability environment.”

The need to move more quickly has been underscored by recent seismic crises, such as the 2009 L’Aquila earthquake sequence, in which an anxious public was confused by informal and inaccurate earthquake predictions. After the L’Aquila earthquake, the Italian Department of Civil Protection appointed an International Commission on Earthquake Forecasting (ICEF), which I chaired, to recommend guidelines for OEF utilization. Our report (Ann. Geophys., 54, 4, 2011; doi: 10.4401/ag-5350) concludes: (a) Public sources of information on short-term probabilities should be authoritative, scientific, open, and timely, and need to convey epistemic uncertainties. (b) Earthquake probabilities should be based on operationally qualified, regularly updated forecasting systems. (c) All operational models should be evaluated for reliability and skill by retrospective testing, and the models should be under continuous prospective testing against long-term forecasts and alternative time-dependent models. (d) Short-term models used in operational forecasting should be consistent with the long-term forecasts used in probabilistic seismic hazard analysis. (e) Alert procedures should be standardized to facilitate decisions at different levels of government, based in part on objective analysis of costs and benefits. (f) In establishing alert protocols, consideration should also be given to the less tangible aspects of value-of-information, such as gains in psychological preparedness and resilience.

Authoritative statements of increased risk, even when the absolute probability is low, can provide a psychological benefit to the public by filling information vacuums that lead to informal predictions and misinformation. Formal OEF procedures based on probabilistic forecasting appropriately separate hazard estimation by scientists from the decision-making role of civil protection authorities. The prosecution of seven Italian scientists on manslaughter charges stemming from their actions before the L’Aquila earthquake makes clear why this separation should be explicit in defining OEF protocols.

Final ID: S21D-05

Coulomb stress changes imparted by simulated M>7 earthquakes to major fault surfaces in Southern California

J. C. Rollins; [1]; *G. P. Ely;* [2, 3]; *T. H. Jordan;* [3];

1. Geophysics, Caltech, Pasadena, CA, United States.
2. Argonne National Laboratory, Chicago, IL, United States.
3. Earth Sciences, University of Southern California, Los Angeles, CA, United States.

Body: To study static stress interactions between faults in southern California and identify cases where one large earthquake could trigger another, we select fourteen M>7 events simulated by the SCEC/CME CyberShake project and calculate the Coulomb stress changes those events impart to major fault surfaces in the UCERF2 fault model for the region. CyberShake simulates between 6 and 32 slip distributions for each event at a slip sampling resolution of 1 km, and we calculate stress changes on fault surfaces at the same resolution, a level of detail which is unprecedented in studies of stress transfer and which allows us to study the way that variabilities in slip on the source can affect imparted stress changes. We find that earthquakes rupturing the southern San Andreas fault generally decrease Coulomb stress on right-lateral faults in the Los Angeles basin, while M>7 events on the San Jacinto, Elsinore, Newport-Inglewood and Palos Verdes faults generally decrease stress on parallel right-lateral faults but increase Coulomb stress on the Mojave or San Bernardino sections of the San Andreas. Stress interactions between strike-slip and thrust faults and between the San Andreas and Garlock faults depend on the rupture area of the source. Coulomb stress changes imparted by simulated SAF events to locations on the San Jacinto and Garlock faults within ~8 km of the San Andreas appear to be influenced more by the nearby distribution of high and low slip on the San Andreas than by the overall slip distribution across the entire rupture. Using a simplified model, we calculate that an area of no slip surrounded by high slip on a rupture imparts strong Coulomb stress increases ≤7 km to either side of the source fault, possibly explaining the apparent ~8-km range of influence of local slip on the San Andreas. Additionally, we devise a method for evaluating uncertainty values in Coulomb stress changes caused by uncertainties in the strike, dip and rake of the receiver fault. These findings may be useful in understanding stress interactions between faults of different orientations and rakes, stress transfer and variability at short distances from the source fault, and applications of uncertainty values to Coulomb stress changes.

Final ID: T22A-06

Earthquake source scaling, stress drops and radiated seismic energies of intermediate depth earthquakes

G. Prieto; [1]; *G. A. Lopez;* [1]; *S. A. Barrett;* [2]; *G. C. Beroza;* [2];

1. Departamento de Física, Universidad de los Andes, Bogota, Colombia.
2. Geophysics, Stanford University, Palo Alto, CA, United States.

Body: The physical mechanism for intermediate and deep focus earthquakes is still under debate. The temperatures and pressures are above the point where ordinary fractures ought to occur. Nevertheless these earthquakes represent a significant portion of global catalogs and various mechanisms have been proposed to explain their presence, including dehydration embrittlement and runaway shear instabilities.

In order to better understand the rupture mechanism it is important to study earthquake source parameters for these events and their scaling behavior with earthquake size as measured by the seismic moment. In this study we analyze rupture area, stress drop and radiated seismic energy for a range of magnitudes and a large number of earthquakes in the Bucaramanga Nest - a concentrated pocket of seismic activity with median depth of 160 km, with more than 15 earthquakes per day - and compare our results with typical values observed for shallow earthquakes.

We study the effect of seismic attenuation and SNR to minimize bias in our estimated source parameters, because the effects of noise and attenuation can lead to lower radiated energy estimates for smaller earthquakes. Preliminary results suggest that the Bucaramanga Nest earthquakes present typical stress drop and apparent stress values, but contrary to their shallow counterparts, they show systematically higher stress drop for larger events.

Final ID: S22A-07

Magnitude Uncertainty and Ground Motion Simulations of the 1811-1812 New Madrid Earthquake Sequence

L. Ramirez Guzman; [1]; *R. W. Graves;* [2]; *K. B. Olsen;* [3]; *O. S. Boyd;* [5]; *S. Hartzell;* [1]; *S. Ni;* [4]; *P. G. Somerville;* [4]; *R. A. Williams;* [1]; *J. Zhong;* [3];

1. Hazards Team, US Geological Survey, Golden, CO, United States.
2. US Geological Survey, Pasadena, CA, United States.
3. San Diego State University, San Diego, CA, United States.
4. URS Corporation, Pasadena, CA, United States.
5. US Geological Survey, Memphis, TN, United States.

Body: We present a study of a set of three-dimensional earthquake simulation scenarios in the New Madrid Seismic Zone (NMSZ). This is a collaboration among three simulation groups with different numerical modeling approaches and computational capabilities. The study area covers a portion of the Central United States (~400,000 km^2) centered on the New Madrid seismic zone, which includes several metropolitan areas such as Memphis, TN and St. Louis, MO. We computed synthetic seismograms to a frequency of 1Hz by using a regional 3D velocity model (Ramirez-Guzman et al., 2010), two different kinematic source generation approaches (Graves et al., 2010; Liu et al., 2006) and one methodology where sources were generated using dynamic rupture simulations (Olsen et al., 2009). The set of 21 hypothetical earthquakes included different magnitudes (Mw 7, 7.6 and 7.7) and epicenters for two faults associated with the seismicity trends in the NMSZ: the Axial (Cottonwood Grove) and the Reelfoot faults. Broad band synthetic seismograms were generated by combining high frequency synthetics computed in a one-dimensional velocity model with the low frequency motions at a crossover frequency of 1 Hz. Our analysis indicates that about 3 to 6 million people living near the fault ruptures would experience Mercalli intensities from VI to VIII if events similar to those of the early nineteenth century occurred today. In addition, the analysis demonstrates the importance of 3D geologic structures, such as the Reelfoot Rift and the Mississippi Embayment, which can channel and focus the radiated wave energy, and rupture directivity effects, which can strongly amplify motions in the forward direction of the ruptures. Both of these effects have a significant impact on the pattern and level of the simulated intensities, which suggests an increased uncertainty in the magnitude estimates of the 1811-1812 sequence based only on historic intensity reports. We conclude that additional constraints such as those provided by paleoliquefaction analyses need to be considered in order to help reduce the magnitude estimate uncertainties.

Final ID: S22A-07

Magnitude Uncertainty and Ground Motion Simulations of the 1811-1812 New Madrid Earthquake Sequence

L. Ramirez Guzman; [1]; *R. W. Graves;* [2]; *K. B. Olsen;* [3]; *O. S. Boyd;* [5]; *S. Hartzell;* [1]; *S. Ni;* [4]; *P. G. Somerville;* [4]; *R. A. Williams;* [1]; *J. Zhong;* [3];

1. Hazards Team, US Geological Survey, Golden, CO, United States.
2. US Geological Survey, Pasadena, CA, United States.
3. San Diego State University, San Diego, CA, United States.
4. URS Corporation, Pasadena, CA, United States.
5. US Geological Survey, Memphis, TN, United States.

Body: We present a study of a set of three-dimensional earthquake simulation scenarios in the New Madrid Seismic Zone (NMSZ). This is a collaboration among three simulation groups with different numerical modeling approaches and computational capabilities. The study area covers a portion of the Central United States (~400,000 km^2) centered on the New Madrid seismic zone, which includes several metropolitan areas such as Memphis, TN and St. Louis, MO. We computed synthetic seismograms to a frequency of 1Hz by using a regional 3D velocity model (Ramirez-Guzman et al., 2010), two different kinematic source generation approaches (Graves et al., 2010; Liu et al., 2006) and one methodology where sources were generated using dynamic rupture simulations (Olsen et al., 2009). The set of 21 hypothetical earthquakes included different magnitudes (Mw 7, 7.6 and 7.7) and epicenters for two faults associated with the seismicity trends in the NMSZ: the Axial (Cottonwood Grove) and the Reelfoot faults. Broad band synthetic seismograms were generated by combining high frequency synthetics computed in a one-dimensional velocity model with the low frequency motions at a crossover frequency of 1 Hz. Our analysis indicates that about 3 to 6 million people living near the fault ruptures would experience Mercalli intensities from VI to VIII if events similar to those of the early nineteenth century occurred today. In addition, the analysis demonstrates the importance of 3D geologic structures, such as the Reelfoot Rift and the Mississippi Embayment, which can channel and focus the radiated wave energy, and rupture directivity effects, which can strongly amplify motions in the forward direction of the ruptures. Both of these effects have a significant impact on the pattern and level of the simulated intensities, which suggests an increased uncertainty in the magnitude estimates of the 1811-1812 sequence based only on historic intensity reports. We conclude that additional constraints such as those provided by paleoliquefaction analyses need to be considered in order to help reduce the magnitude estimate uncertainties.

Final ID: IN23B-1448

SCEC Broadband Platform Strong Ground Motion Simulations

S. Kumar; [1]; *S. Callaghan;* [1]; *P. J. Maechling;* [1]; *K. B. Olsen;* [2]; *R. J. Archuleta;* [3]; *P. G. Somerville;* [4]; *R. W. Graves;* [5]; *T. H. Jordan;* [1];

1. Southern California Earthquake Center, University of Southern California, Los Angeles, CA, United States.
2. Geological Sciences, San Diego State University, San Diego, CA, United States.
3. Earth Science, University of California, Santa Barbara, Santa Barbara, CA, United States.
4. URS Corporation, Pasadena, CA, United States.
5. Earthquake Science Center, U.S. Geological Survey, Pasadena, CA, United States.

Body: The Southern California Earthquake Center (SCEC) Broadband Platform is a collaborative software development project involving SCEC researchers, graduate students, and the SCEC Community Modeling Environment. The goal of the SCEC Broadband Simulation Platform is to generate broadband (0-10 Hz) ground motions for earthquakes using deterministic low-frequency and stochastic high-frequency simulations. SCEC developers have integrated complex scientific modules for rupture generation, low-frequency deterministic seismogram synthesis, high-frequency stochastic seismogram synthesis, and non-linear site effects calculation into a system that supports easy on-demand computation of broadband seismograms. The SCEC Broadband platform has two primary modes of operation, validation mode, and scenario mode. In validation mode, the earthquake modeling software calculates broadband seismograms for one of three earthquakes, Northridge, Loma Prieta, or Landers at sites with observed strong motion data. Then, the platform calculates goodness of fit measurements that quantify how well the model-based broadband seismograms match the observed seismograms for each event. In scenario mode, the user can specify a scenario earthquake and a list of sites and calculate ground motions at each site for the scenario event. In February 2011, SCEC released Broadband Platform 11.2 as an open-source scientific software distribution. Since that time, we have continued development of the platform by adding a new site response module and new goodness of fit measures by Mayhew and Olsen. Along with a source code distribution of the Broadband Platform, we now offer a virtual software image distribution of the platform to support its use on a variety of computing hardware and operating systems.

Final ID: IN23B-1451

New developments and applicability of the Collaboratory for the Study of Earthquake Predictability (CSEP) testing framework

M. Liukis; [1]; *D. Schorlemmer;* [1]; *J. Yu;* [1]; *P. J. Maechling;* [1]; *J. D. Zechar;* [2]; *T. H. Jordan;* [1];

1. Southern California Earthquake Center, USC, Los Angeles, CA, United States.
2. Schweiz. Erdbebendienst (SED), ETH, Zurich, Switzerland.

Body: Southern California Earthquake Center (SCEC) began development of the Collaboratory for the Study of Earthquake Predictability (CSEP) in January of 2006 with funding provided by the W. M. Keck Foundation. Since that time, scientists and software engineers have applied the scientific and computational principles of CSEP to develop several operational testing centers. The W. M. Keck Foundation Testing Center at SCEC, designed to conduct computational earthquake forecast experiments in California, began operations on September 1, 2007 and has been improved, optimized, and extended over the past four years. The implementation of the SCEC Testing Center has been guided by four design goals proposed by the Regional Earthquake Likelihood Models (RELM) working group: (1) Controlled Environment, (2) Transparency, (3) Comparability, and (4) Reproducibility. By meeting these goals, the CSEP testing framework can provide clear descriptions of how all registered earthquake forecasts are produced and evaluated. As of August 2011, there are four testing centers established around the globe, with 224 models under test. CSEP software is also available for personal use by scientists to perform independent study and evaluation of their model prior submitting it to the Testing Center (http://northridge.usc.edu/trac/csep/wiki/MiniCSEP). The SCEC Testing Center hosts intermediate-term and short-term alarm-based and rate-based forecasts for California, the Western Pacific, and a global testing region. We describe how the CSEP Testing Center at SCEC has been constructed to meet the design goals; we also present recent developments of the Testing Center and share our experiences operating the center since its inception. Additionally, we discuss how the CSEP infrastructure is now being applied to geodetic transient detection and earthquake early warning experiments.

Final ID: S23B-2271

Search for Non-Volcanic Tremor in the Aftermath of the 2010 M8.8 Maule, Chile Earthquake

R. J. Walters; [1]; *G. C. Beroza;* [1]; *S. Ide;* [2];

1. Geophysics, Stanford University, Stanford, CA, United States.
2. Earth and Planetary Science, University of Tokyo, Tokyo, Japan.

Body: We seek to understand the relationship between the areal extent of non-volcanic tremor and seismic slip in large subduction zone events. Ideally, we would study areas where tremor is known to occur, and where the slip distribution in a large earthquake is well known; however, the subduction zones with the best constraints on tremor locations - Cascadia and the Nankai Trough - have not suffered recent large earthquakes. We attempt to study this relationship by searching for tremor using seismic data from the Chile IRIS RAMP network that was deployed following the February 27, 2010 M 8.8 Maule, Chile earthquake. The Chile RAMP network collected data between mid-March 2010 to the end of September 2010 in the region surrounding the epicenter of the event. Although non-volcanic tremor has not yet been reported near the Maule mainshock zone, it may have been observed to the north of the Chile Triple Junction (Gallego et al, 2006). We apply waveform envelope analysis to the RAMP data, and because of the sensitivity of this approach to aftershocks, we concentrate on data towards the end of the deployment. By identifying any possible non-volcanic tremor in the South American subduction zone, we hope to better understand if there is a relationship between tremor and mainshock slip.

Final ID: S23B-2271

Search for Non-Volcanic Tremor in the Aftermath of the 2010 M8.8 Maule, Chile Earthquake

R. J. Walters; [1]; *G. C. Beroza;* [1]; *S. Ide;* [2];

1. Geophysics, Stanford University, Stanford, CA, United States.
2. Earth and Planetary Science, University of Tokyo, Tokyo, Japan.

Body: We seek to understand the relationship between the areal extent of non-volcanic tremor and seismic slip in large subduction zone events. Ideally, we would study areas where tremor is known to occur, and where the slip distribution in a large earthquake is well known; however, the subduction zones with the best constraints on tremor locations - Cascadia and the Nankai Trough - have not suffered recent large earthquakes. We attempt to study this relationship by searching for tremor using seismic data from the Chile IRIS RAMP network that was deployed following the February 27, 2010 M 8.8 Maule, Chile earthquake. The Chile RAMP network collected data between mid-March 2010 to the end of September 2010 in the region surrounding the epicenter of the event. Although non-volcanic tremor has not yet been reported near the Maule mainshock zone, it may have been observed to the north of the Chile Triple Junction (Gallego et al, 2006). We apply waveform envelope analysis to the RAMP data, and because of the sensitivity of this approach to aftershocks, we concentrate on data towards the end of the deployment. By identifying any possible non-volcanic tremor in the South American subduction zone, we hope to better understand if there is a relationship between tremor and mainshock slip.

Final ID: S23B-2276

Auto-correlation Clustering Event Detection Applied to Tectonic Tremor

A. C. Aguiar; [1]; *G. C. Beroza;* [1];

1. Geophysics, Stanford, Stanford, CA, United States.

Body: We exploit the fact that tectonic tremor has been shown to be comprised of frequently occurring and repeating low frequency earthquakes (LFEs) to identify those events. We refer to this approach as the auto-correlation clustering detection method because it builds on the auto-correlation approach of Brown et al. (2008) which detects events based on pair-wise matching. Our method takes advantage of the fact that common signals repeat many times within the tremor signal. This method is applied to 24 hours of data during the April, 2006 tremor episode in the Nankai Trough in SW Japan. We analyze 1-hour periods at a time by auto-correlating 8 s windows shifted 2 samples each. We then shift 20 minutes ahead of the previously analyzed hour and carry detections until the 24 hours of data are completed. We apply a 3-sigma detection threshold to find individual matches, then tally the number of detections for each window and use this as our test statistic. For band-limited Gaussian white noise, the number of detections should follow a binomial distribution governed by the assumed detection threshold. We use this null hypothesis to test the significance of the detection of a candidate LFE family. Our method places the detection of LFE families on a sound statistical basis. It should improve our ability to detect LFEs within weak tremor signals and will likely be applicable to other earthquake swarms.

Final ID: U23C-05

Tracking Earthquake Cascades *(Invited)*

T. H. Jordan; [1];

1. Dept of Earth Sciences ZHS-169, Univ of Southern California, Los Angeles, CA, United States.

Body: In assessing their risk to society, earthquakes are best characterized as cascades that can propagate from the natural environment into the socio-economic (built) environment. Strong earthquakes rarely occur as isolated events; they usually cluster in foreshock-mainshock-aftershock sequences, seismic swarms, and extended sequences of large earthquakes that propagate along major fault systems. These cascades are regulated by stress-mediated interactions among faults driven by tectonic loading. Within these cascades, each large event can itself cause a chain reaction in which the primary effects of faulting and ground shaking induce secondary effects, including tsunami, landslides, liquefaction, and set off destructive processes within the built environment, such as fires and radiation leakage from nuclear plants. Recent earthquakes have demonstrated how the socio-economic effects of large earthquakes can reverberate for many years.

To reduce earthquake risk and improve the resiliency of communities to earthquake damage, society depends on five geotechnologies for tracking earthquake cascades: long-term probabilistic seismic hazard analysis (PSHA), short-term (operational) earthquake forecasting, earthquake early warning, tsunami warning, and the rapid production of post-event information for response and recovery (see figure). In this presentation, I describe how recent advances in earthquake system science are leading to improvements in this geotechnology pipeline. In particular, I will highlight the role of earthquake simulations in predicting strong ground motions and their secondary effects before and during earthquake cascades

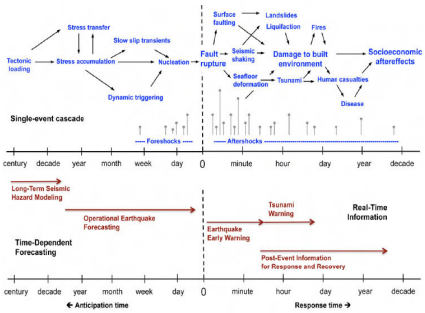

Single-event earthquake cascade showing five geotechnologies useful for anticipating and responding to events during the casacde. Zero time is the origin time of the earthquake.

Final ID: S31A-2214

Application of Second-Moment Source Analysis to Three Problems in Earthquake Forecasting

J. Donovan; [1]; *T. H. Jordan;* [1];

1. Earth Sciences, Univ. of Southern California, Los Angeles, CA, United States.

Body: Though earthquake forecasting models have often represented seismic sources as space-time points (usually hypocenters), a more complete hazard analysis requires the consideration of finite-source effects, such as rupture extent, orientation, directivity, and stress drop. The most compact source representation that includes these effects is the finite moment tensor (FMT), which approximates the degree-two polynomial moments of the stress glut by its projection onto the seismic (degree-zero) moment tensor. This projection yields a scalar space-time source function whose degree-one moments define the centroid moment tensor (CMT) and whose degree-two moments define the FMT. We apply this finite-source parameterization to three forecasting problems. The first is the question of hypocenter bias: can we reject the null hypothesis that the conditional probability of hypocenter location is uniformly distributed over the rupture area? This hypothesis is currently used to specify rupture sets in the “extended” earthquake forecasts that drive simulation-based hazard models, such as CyberShake. Following McGuire et al. (2002), we test the hypothesis using the distribution of FMT directivity ratios calculated from a global data set of source slip inversions. The second is the question of source identification: given an observed FMT (and its errors), can we identify it with an FMT in the complete rupture set that represents an extended fault-based rupture forecast? Solving this problem will facilitate operational earthquake forecasting, which requires the rapid updating of earthquake triggering and clustering models. Our proposed method uses the second-order uncertainties as a norm on the FMT parameter space to identify the closest member of the hypothetical rupture set and to test whether this closest member is an adequate representation of the observed event. Finally, we address the aftershock excitation problem: given a mainshock, what is the spatial distribution of aftershock probabilities? The FMT representation allows us to generalize the models typically used for this purpose (e.g., marked point process models, such as ETAS), which will again be necessary in operational earthquake forecasting. To quantify aftershock probabilities, we compare mainshock FMTs with the first and second spatial moments of weighted aftershock hypocenters. We will describe applications of these results to the Uniform California Earthquake Rupture Forecast, version 3, which is now under development by the Working Group on California Earthquake Probabilities.

Final ID: S31G-05

Discriminating Tectonic Tremor from Magmatic Processes in Observationally Challenging Environments

J. R. Brown; [1]; *G. C. Beroza;* [1];

1. Geophysics, Stanford University, Stanford, CA, United States.

Body: Deep tectonic tremor is a long-duration, low amplitude signal that has been shown to consist of low frequency earthquakes (LFEs) on the plate interface in subduction zones. Detecting LFEs from tremor-like signals in subduction settings can be challenging due to the combination of volcanic seismicity and sparse station geometry. This is particularly true for island arcs such as the Alaska-Aleutian subduction zone where the islands are small and noise levels are high. We have detected and located LFEs within tremor signals along the Alaska-Aleutian Arc in four locations: Kodiak Island, Alaska Peninsula, eastern Aleutians, and the Andreanof Islands. In all areas, the LFEs are located 10-40 km trenchward of the volcanic chain at depths ranging from 45-70 km. Location errors are significant (+/- 20 km in depth) due to sparse station geometry such that there is the possibility that the tremor could be associated with nearby volcanoes. Since most documented volcanic tremor is located in the shallow crust, it can often be discriminated from tectonic tremor simply based on location. However, deep volcanic tremor has been documented in Hawaii to depths of 40 km and could be more widespread. In the Aleutian arc, deep long period events (DLPs), which are thought to result from the movement of magma and volatiles, have been located as deep as 45 km and sometimes resemble tremor-like signals.

The spectral character is another potential discriminant. We compare the cepstra (Fourier transform of the logarithmic power spectrum of a time series) of the tectonic tremor-like signals/LFEs and DLPs associated with volcanoes. Source characteristics of DLPs (non-shear slip) and tectonic tremor/LFEs (shear slip) are distinct and should be noticeable in the cepstral domain. This approach of using tremor locations and cepstral analysis could be useful for detecting and differentiating tectonic tremor from deep volcanic processes in other island arcs as well.

Final ID: U41D-07

Shaking and flooding by the Tohoku-Oki Earthquake

S. Wei; [1]; *D. V. Helmberger;* [1]; *R. W. Graves;* [2]; *H. Kanamori;* [1]; *J. Avouac;* [1];

1. Geological and Planetary Sciences, Caltech, Pasadena, CA, United States.
2. USGS, Pasadena, CA, United States.

Body: Large subduction zone earthquakes pose one of the greatest nature hazards to mankind, either by shaking down structures and/or flooding. Rupture properties of these rare events are poorly understood, especially tsunamigenic earthquakes with little pre-shaking such as the 1896 Sanriku earthquake. The well recorded Tohoku-Oki earthquake sheds some new light on these issues. Here we document the history of the rupture from the inversion of accelerometric waveform data and high-rate GPS data. Our results demonstrate that the flooding was caused by the shallow ruptured (Mw~9) portion close to the trench while the shaking came from ruptures at depth >30km with a relatively small magnitude (Mw~8.5). Several deep pockets of high frequency energy release can be resolved, which correspond to locations predicted from back-projection. The Peak Ground Velocity (PGV) recorded by over 1400 strong motions and ~400 high rate GPS stations is nicely correlated with geological structure (topography). Separation of the wavefield into upgoing and downgoing energy indicates that the shaking on the island is mainly controlled by upgoing energy. Forward calculation indicates that the shallow basin structure could amplify the ground shaking and some of the high frequency arrivals could be explained by using a modified source time function which suggests a pulse like rupture.

Final ID: T42A-06

A Discrete Element Modeling Approach to Exploring the Transition Between Fault-related Folding Styles

A. N. Hughes; [1]; *N. P. Benesh;* [1]; *R. C. Alt II;* [1]; *J. H. Shaw;* [1];

1. Department of Earth and Planetary Sciences, Harvard University, Cambridge, MA, United States.

Body: Contractional fault-related folds form as stratigraphic layers of rock are deformed due to displacement on an underlying fault. Specifically, fault-bend folds form as rock strata are displaced over non-planar faults, and fault-propagation folds form at the tips of faults as they propagate upward through sedimentary layers. Both types of structures are commonly observed in fold and thrust belts and passive margin settings throughout the world. Fault-bend and fault-propagation folds are often seen in close proximity to each other, and kinematic analysis of some fault-related folds suggests that they have undergone a transition in structural style from fault-bend to fault-propagation folding during their deformational history. Because of the similarity in conditions in which both fault-bend and fault-propagation folds are found, the circumstances that promote the formation of one of these structural styles over the other is not immediately evident.

In an effort to better understand this issue, we have investigated the role of mechanical and geometric factors in the transition between fault-bend folding and fault-propagation folding using a series of models developed with the discrete element method (DEM). The DEM models employ an aggregate of circular, frictional disks that incorporate bonding at particle contacts to represent the numerical stratigraphy. A vertical wall moving at a fixed velocity drives displacement of the hanging-wall section along a pre-defined fault ramp and detachment. We utilize this setup to study the transition between fault-bend and fault-propagation folding by varying mechanical strength, stratigraphic layering, fault geometries, and boundary conditions of the model.

In most circumstances, displacement of the hanging-wall leads to the development of an emergent fold as the hanging-wall material passes across the fault bend. However, in other cases, an emergent fault propagates upward through the sedimentary section, associated with the development of a steep, narrow front-limb, characteristic of fault-propagation folding. We find that the boundary conditions imposed on the far wall of the model have the strongest influence on structural style, but that other factors, such as fault dip and mechanical strengths, play secondary roles. By testing a range of values for each of the parameters, we are able to identify the range of values under which the transition occurs. Additionally, we find that the transition between fault-bend and fault-propagation folding is gradual, with structures in the transitional regime showing evidence of each structural style during a portion of their history.

The primary role that boundary conditions play in determining fault-related folding style implies that the growth of natural structures may be affected by the emergence of adjacent structures, or in distal variations in detachment strengths. We explore these relationships using natural examples from various fold-and-thrust belts.

Final ID: T42A-06

A Discrete Element Modeling Approach to Exploring the Transition Between Fault-related Folding Styles

A. N. Hughes; [1]; *N. P. Benesh;* [1]; *R. C. Alt II;* [1]; *J. H. Shaw;* [1];

1. Department of Earth and Planetary Sciences, Harvard University, Cambridge, MA, United States.

Body: Contractional fault-related folds form as stratigraphic layers of rock are deformed due to displacement on an underlying fault. Specifically, fault-bend folds form as rock strata are displaced over non-planar faults, and fault-propagation folds form at the tips of faults as they propagate upward through sedimentary layers. Both types of structures are commonly observed in fold and thrust belts and passive margin settings throughout the world. Fault-bend and fault-propagation folds are often seen in close proximity to each other, and kinematic analysis of some fault-related folds suggests that they have undergone a transition in structural style from fault-bend to fault-propagation folding during their deformational history. Because of the similarity in conditions in which both fault-bend and fault-propagation folds are found, the circumstances that promote the formation of one of these structural styles over the other is not immediately evident.

In an effort to better understand this issue, we have investigated the role of mechanical and geometric factors in the transition between fault-bend folding and fault-propagation folding using a series of models developed with the discrete element method (DEM). The DEM models employ an aggregate of circular, frictional disks that incorporate bonding at particle contacts to represent the numerical stratigraphy. A vertical wall moving at a fixed velocity drives displacement of the hanging-wall section along a pre-defined fault ramp and detachment. We utilize this setup to study the transition between fault-bend and fault-propagation folding by varying mechanical strength, stratigraphic layering, fault geometries, and boundary conditions of the model.

In most circumstances, displacement of the hanging-wall leads to the development of an emergent fold as the hanging-wall material passes across the fault bend. However, in other cases, an emergent fault propagates upward through the sedimentary section, associated with the development of a steep, narrow front-limb, characteristic of fault-propagation folding. We find that the boundary conditions imposed on the far wall of the model have the strongest influence on structural style, but that other factors, such as fault dip and mechanical strengths, play secondary roles. By testing a range of values for each of the parameters, we are able to identify the range of values under which the transition occurs. Additionally, we find that the transition between fault-bend and fault-propagation folding is gradual, with structures in the transitional regime showing evidence of each structural style during a portion of their history.

The primary role that boundary conditions play in determining fault-related folding style implies that the growth of natural structures may be affected by the emergence of adjacent structures, or in distal variations in detachment strengths. We explore these relationships using natural examples from various fold-and-thrust belts.

Final ID: S43C-2258

Rupture behavior and ground motion from 3D simulations of the Casa Loma – Claremont stepover on the San Jacinto Fault, southern California

J. Lozos; [1]; *D. D. Oglesby;* [1]; *J. N. Brune;* [2]; *K. B. Olsen;* [3];

1. Department of Earth Sciences, UC Riverside, Riverside, CA, United States.
2. Department of Geological Sciences, University of Nevada, Reno, NV, United States.
3. Department of Geological Sciences, San Diego State University, San Diego, CA, United States.

Body: The extensional stepover between the Claremont and Casa Loma strands of the San Jacinto Fault in southern California is an area in which complex fault geometry may have a controlling effect on both rupture propagation and ground motion. The two main strands of the fault in this region are roughly parallel, with an average 4 km separation between them, but smaller complexities within the individual strands may affect rupture velocity, slip rate, seismic radiation, and ground motion. The presence of the Farm Road strand, a smaller fault segment between the Claremont and Casa Loma strands, may add further complexity to the rupture behavior. We use the three-dimensional finite element method to conduct models of this complex stepover region. We test several different nucleation locations, several initial stress states, and several different seismogenic depths for the Farm Road strand. We then use the outputs of these dynamic models to determine ground motion distributions from these ruptures. We find that the nucleation location strongly affects the rupture's ability to jump the stepover; nucleations closer to the overlap are less likely to result in jumping rupture. Including the Farm Road strand makes a considerable difference in the rupture behavior and ground motion distribution when compared to a model without it, though its contribution is complex. The strength of its effect is variable based on nucleation location, and while its presence does allow rupture to jump the larger stepover in stress states that would normally prohibit jumping, it serves to reduce radiated energy and ground motion in stress states that would allow rupture to jump in the absence of the smaller strand. The depth of the Farm Road strand has more effect on the rupture in the stress state that would not permit jumping in the absence of that segment. These results suggest that hazard associated with rupture on the northern San Jacinto depends on specific nucleation point, but also that a seemingly less-permissive stress state for throughgoing rupture may ultimately lead to stronger ground motions. This work also continues to highlight the non-monotonic effects of an intermediate fault segment on rupture behavior through a larger stepover.

Final ID: S43C-2258

Rupture behavior and ground motion from 3D simulations of the Casa Loma – Claremont stepover on the San Jacinto Fault, southern California

J. Lozos; [1]; *D. D. Oglesby;* [1]; *J. N. Brune;* [2]; *K. B. Olsen;* [3];

1. Department of Earth Sciences, UC Riverside, Riverside, CA, United States.
2. Department of Geological Sciences, University of Nevada, Reno, NV, United States.
3. Department of Geological Sciences, San Diego State University, San Diego, CA, United States.

Body: The extensional stepover between the Claremont and Casa Loma strands of the San Jacinto Fault in southern California is an area in which complex fault geometry may have a controlling effect on both rupture propagation and ground motion. The two main strands of the fault in this region are roughly parallel, with an average 4 km separation between them, but smaller complexities within the individual strands may affect rupture velocity, slip rate, seismic radiation, and ground motion. The presence of the Farm Road strand, a smaller fault segment between the Claremont and Casa Loma strands, may add further complexity to the rupture behavior. We use the three-dimensional finite element method to conduct models of this complex stepover region. We test several different nucleation locations, several initial stress states, and several different seismogenic depths for the Farm Road strand. We then use the outputs of these dynamic models to determine ground motion distributions from these ruptures. We find that the nucleation location strongly affects the rupture's ability to jump the stepover; nucleations closer to the overlap are less likely to result in jumping rupture. Including the Farm Road strand makes a considerable difference in the rupture behavior and ground motion distribution when compared to a model without it, though its contribution is complex. The strength of its effect is variable based on nucleation location, and while its presence does allow rupture to jump the larger stepover in stress states that would normally prohibit jumping, it serves to reduce radiated energy and ground motion in stress states that would allow rupture to jump in the absence of the smaller strand. The depth of the Farm Road strand has more effect on the rupture in the stress state that would not permit jumping in the absence of that segment. These results suggest that hazard associated with rupture on the northern San Jacinto depends on specific nucleation point, but also that a seemingly less-permissive stress state for throughgoing rupture may ultimately lead to stronger ground motions. This work also continues to highlight the non-monotonic effects of an intermediate fault segment on rupture behavior through a larger stepover.

Final ID: U51B-0032

Shallow Dynamic Overshoot and Energetic Deep Rupture in the 2011 Mw 9.0 Tohoku-Oki Earthquake

S. Ide; [1]; *A. Baltay;* [2]; *S. Tamura;* [1]; *G. C. Beroza;* [2];

1. Dept. Earth & Planetary Sci., University of Tokyo, Tokyo, Japan.
2. Dept. Geophysics, Stanford University, Stanford, CA, United States.

Body: We use empirical Green's function-based finite-source imaging and energy estimates to study rupture evolution of the Mw 9.0 Tohoku-Oki earthquake. The earthquake consists of: (1) a small initial phase of about 3 s, (2) deep rupture up to 40 s, (3) extensive shallow rupture at 60-70 s, and (4) continuing deep rupture lasting over 100 s. Exceptionally high values of shallow slip near the trench may have been enabled by a combination of a shallow dipping fault and a compliant hanging wall. The transition of rupture propagation direction from upward to downward is also the result of interaction of rupture with the free surface. Extreme dynamic overshoot on the fault is supported by low-angle normal faulting aftershocks on the plate interface in the area of high slip. Despite prodigious total slip, shallower parts of the rupture radiated only weakly at high frequencies, whereas deeper parts of the rupture radiated strongly at high frequencies, making this event ordinary in terms of overall seismic energy radiation. The azimuthal dependence of seismic energy estimates is consistent with the slip model, with the overall maximum at around 300° and two sharp peaks corresponding to the sudden emergence of large slip along the trench.

The Tohoku-Oki earthquake has two modes of rupture: shallow, relatively quiet rupture with dynamic overshoot and deep rupture that radiates high frequency waves energetically. Observations at either high or low frequencies alone would result in a misleading representation of the earthquake. Our observations suggest that the two rupture modes of the Tohoku-Oki earthquake reflect variations in the frictional nature of the subduction interface with depth, and may explain variable earthquake behavior in the Japan Trench.

Final ID: NH51B-1696

Broadband CyberShake Platform: Seismogram Synthesis for Broadband Physics-Based Probabilistic Seismic Hazard Analysis

S. Callaghan; [1]; *P. J. Maechling;* [1]; *P. Small;* [1]; *K. Milner;* [1]; *R. W. Graves;* [2]; *T. H. Jordan;* [1];
1. Southern California Earthquake Center, University of Southern California, Los Angeles, CA, United States.
2. USGS, Pasadena, CA, United States.

Body: Researchers at the Southern California Earthquake Center (SCEC) have developed the CyberShake computational platform to perform probabilistic seismic hazard analysis (PSHA) in the Los Angeles region (Graves et al., 2010) using deterministic wave propagation simulations at frequencies up to 0.5 Hz. CyberShake uses seismic reciprocity to calculate synthetic seismograms for a suite of more than 600,000 rupture realizations. From this set of seismograms we compute intensity measures, which are then combined into a PSHA hazard curve for the site of interest.

SCEC has also developed the SCEC Broadband Ground Motion Simulation Platform, a software system that can calculate broadband seismograms at frequencies up to 10 Hz for historical and scenario earthquakes using multiple earthquake rupture generators, multiple low- and high-frequency wave propagation simulation codes, and multiple site effects modules.

Here we report how we have integrated the high-frequency computational capabilities of the SCEC Broadband Platform into CyberShake, producing the Broadband CyberShake Platform. The Broadband CyberShake Platform extends the frequency range up to 10 Hz by combining low frequency deterministic synthetic seismograms with higher frequency stochastic seismograms. We can now calculate physics-based seismograms and PSHA hazard curves for intensity measures such as PGA that are strongly dependent on higher frequency ground motions. A potential benefit of this approach, particularly at higher frequencies, is that given adequate sampling of the parameter space, the physics-based model naturally limits the upper bound of the estimated ground motion response. This often leads to a reduction in hazard at longer return periods.

We are applying the computational capabilities of the SCEC Broadband CyberShake Platform at southern California sites selected to support validation of this newly developed PSHA computational technique. This includes calculation of Broadband CyberShake seismograms at Southern California Seismic Network station locations for comparison with observations for well-observed Southern California earthquakes, as well as calculation of Broadband CyberShake hazard curves at precariously balanced rock sites to validate our technique and to investigate the impact of higher frequencies on these fragile geological structures.

Final ID: DI51A-2119

Global Correlations of Mantle Structure with Crustal Tectonic Regions

E. Paulson; [1]; *T. H. Jordan;* [1];

1. Department of Earth Sciences, University of Southern California, Los Angeles, CA, United States.

Body: Tomographic models of Earth's mantle depend on a priori estimates of crustal elastic structure, but the model prior is usually independent of other structural information about the crust, such as geochronological age and tectonic history. Therefore, the correlation of mantle models with crustal structure can provide powerful insights about the relationship of mantle heterogeneity to lithospheric dynamics and continental evolution. In a meta-analysis of more than 20 whole-mantle tomographic models published by various research groups, we estimate the correlation between upper-mantle seismic structure and crustal tectonic structure by projecting the tomographic models onto the GTR1 global tectonic regionalization. The 5 x 5 degree GTR1 map comprises three continental regions based on generalized tectonic behavior during the Phanerozoic: S (Precambrian shields and platforms), P (Phanerozoic platforms), Q (Phanerozoic orogenic zones); as well as three oceanic regions based on crustal age: A (0-25 Ma), B (25-100 Ma), and C (>100 Ma). We computed shear-velocity perturbation profiles by averaging a tomographic model over each of the six tectonic regions. For each model, we assessed the statistical significance of the inter-regional variations at a fixed depth by computing the intra-regional variance and correlation length. The regionalized velocity profiles of the upper mantle are similar among all of the tomographic models that we analyzed. Within the oceanic regions, the models display a consistent increase of shear velocity with crustal age that remains statistically significant to a depth of 200 km. The oceanic shear-velocity variations are consistent with high-resolution models derived from anisotropic inversions of multi-phase waveform data in localized regions. The profiles for regions S and P show consistent and statistically significant cratonic signatures extending below 300 km depth. In particular, the shear velocity gradients of both regions are distinctly lower than those of the convecting oceanic mantle in the depth interval 200-400 km, which also agrees with high-resolution models derived for specific cratons.

Final ID: S51B-2214

Directivity-Basin Coupling in the Los Angeles Region from the CyberShake Hazard Model

F. Wang; [1]; *T. H. Jordan;* [1]; *S. Callaghan;* [1]; *K. Milner;* [1]; *P. J. Maechling;* [1]; *R. W. Graves;* [2];

1. Earth Sciences, Uni. of Southern California, Los Angeles, CA, United States.
2. US Geological Survey, Golden, CO, United States.

Body: The coupling between source directivity effects and basin amplification effects can substantially enhance the low-frequency seismic hazards in sedimentary basins. These effects have been qualitatively illustrated by TeraShake (Olsen et al., 2006), ShakeOut (Graves et al., 2008), and other earthquake scenarios simulated by the Southern California Earthquake Center. In this study, we use version 1 of the CyberShake Hazard Model (CSHM-1) for the Los Angeles region (Graves et al., 2010) to quantify directivity-basin effects in low-frequency response spectra. The CyberShake computational platform employs the reversal symmetries of linear wave propagation (seismic reciprocity) to numerically simulate suites of synthetic time-histories large enough for the probabilistic mapping of shaking intensities. In CSHM-1, a set of more than 600,000 rupture realizations was generated that stochastically sample the Uniform California Earthquake Rupture Forecast (UCERF2); horizontal-component seismograms were computed at 250 sites in the Los Angeles region, and hazard curves and hazard maps were constructed from the UCERF2 probabilities. We use the response spectra calculated from these seismograms in the band 0.1-0.3 Hz to analyze the dependence of strong-motion amplitudes on basin and source geometry, from which we extract measures of directivity-basin coupling. These measures indicate how directivity-basin coupling is enhanced by the tectonic branching structure of the San Andreas system. We analyze the dependence of this coupling on source complexity and earth structure, and we compare our results with parameterizations of basin and directivity effects in the ground motion prediction equations of the Next Generation Attenuation Project (2008).

Final ID: S51B-2215

A Unified Finite Element Method for Arbitrary Elastic and Acoustic Media

H. Karaoglu; [1]; *J. Bielak;* [1];
1. Carnegie Mellon University, Pittsburgh, PA, United States.

Body: This study reports on a mixed finite element formulation that overcomes certain limitations faced by low-order primal-based formulations.
A primal-based formulation with displacement as the variable is a widely used method to solve wave-propagation problems. It has been observed, however, that its accuracy deteriorates badly with increasing contrast between the P- and S-wave velocities (a situation often referred to, inaccurately, as almost incompressible). The extreme case for this contrast is an ideal, compressible fluid medium with S-wave velocity equals to zero. This extreme case creates problems in the equations of compressible elasticity.
By using a dual-based formulation, we develop a method that is robust within the entire range of an elastic solid with moderate contrast between the P- and S-wave velocities up to
the limiting case of an acoustic medium for which the S-wave velocity is zero. By solving a constrained variational problem with the Lagrange-Multiplier Method, we developed the dual-based (mixed) formulation with pressure and displacement as the variables.This is similar to
earlier mixed displacement-pressure formulations, except that we introduce the methodology as a global one applicable to different domains rather than being limited to certain extreme cases. The variational problem makes a wider range of interpolation functions permissible for
pressure including discontinuous functions across element boundaries.
We verify the method and illustrate the general principles with an application in Southern California of the 1994 Northridge earthquake.
We also discuss the possible extension of the method to fluid-structure interaction problems with dry interface conditions.

Final ID: S51B-2215

A Unified Finite Element Method for Arbitrary Elastic and Acoustic Media

H. Karaoglu; [1]; *J. Bielak;* [1];
1. Carnegie Mellon University, Pittsburgh, PA, United States.

Body: This study reports on a mixed finite element formulation that overcomes certain limitations faced by low-order primal-based formulations.
A primal-based formulation with displacement as the variable is a widely used method to solve wave-propagation problems. It has been observed, however, that its accuracy deteriorates badly with increasing contrast between the P- and S-wave velocities (a situation often referred to, inaccurately, as almost incompressible). The extreme case for this contrast is an ideal, compressible fluid medium with S-wave velocity equals to zero. This extreme case creates problems in the equations of compressible elasticity.
By using a dual-based formulation, we develop a method that is robust within the entire range of an elastic solid with moderate contrast between the P- and S-wave velocities up to
the limiting case of an acoustic medium for which the S-wave velocity is zero. By solving a constrained variational problem with the Lagrange-Multiplier Method, we developed the dual-based (mixed) formulation with pressure and displacement as the variables.This is similar to
earlier mixed displacement-pressure formulations, except that we introduce the methodology as a global one applicable to different domains rather than being limited to certain extreme cases. The variational problem makes a wider range of interpolation functions permissible for
pressure including discontinuous functions across element boundaries.
We verify the method and illustrate the general principles with an application in Southern California of the 1994 Northridge earthquake.
We also discuss the possible extension of the method to fluid-structure interaction problems with dry interface conditions.

Final ID: S51C-2244

Station-to-Station Green's Functions Extracted From Seismic Coda in Southern California

E. T. Hirakawa; [1, 2]; *S. Ma;* [1];

1. Department of Geological Sciences, San Diego State University, San Diego, CA, United States.
2. Scripps Insitution of Oceanography, IGPP, University of California, San Diego, La Jolla, CA, United States.

Body: It has been demonstrated recently that correlation of seismic diffuse field (ambient noise and coda) recorded at two stations leads to deterministic station-to-station Green's functions. The theory requires a homogeneous distribution of uncorrelated sources or scatters. However, this condition is not satisfied by the ambient noise data, which is dominated by the microseisms. In this study, we will explore the seismic coda recorded in southern California for over 10 years. In contrary to ambient seismic noise, coda waves, generated by multiple scattering by small-scale heterogeneities, are independent of the sources that generate them. The Green's function extracted from coda waves should approach more closely to the true Green's functions. These Green's functions will provide a way to quantify the bias in these two different data sets. We will also explore the frequency content and amplitude of coda-wave Green's functions and compare them with numerical Green's functions based on the current Community Velocity Models of southern California.

Final ID: S51C-2244

Station-to-Station Green's Functions Extracted From Seismic Coda in Southern California

E. T. Hirakawa; [1, 2]; *S. Ma;* [1];

1. Department of Geological Sciences, San Diego State University, San Diego, CA, United States.
2. Scripps Insitution of Oceanography, IGPP, University of California, San Diego, La Jolla, CA, United States.

Body: It has been demonstrated recently that correlation of seismic diffuse field (ambient noise and coda) recorded at two stations leads to deterministic station-to-station Green's functions. The theory requires a homogeneous distribution of uncorrelated sources or scatters. However, this condition is not satisfied by the ambient noise data, which is dominated by the microseisms. In this study, we will explore the seismic coda recorded in southern California for over 10 years. In contrary to ambient seismic noise, coda waves, generated by multiple scattering by small-scale heterogeneities, are independent of the sources that generate them. The Green's function extracted from coda waves should approach more closely to the true Green's functions. These Green's functions will provide a way to quantify the bias in these two different data sets. We will also explore the frequency content and amplitude of coda-wave Green's functions and compare them with numerical Green's functions based on the current Community Velocity Models of southern California.

Final ID: T51C-2347

Incorporating fault-slip constraints in 3D geomechanical restoration with application to restraining bend systems in the deep-water Niger Delta.

P. Durand-Riard; [1]; *J. H. Shaw;* [1]; *A. Plesch;* [1];

1. Department of Structural Geology and Earth Resources, Harvard University, Cambridge, MA, United States.

Body: In the past few years, geomechanical restoration has emerged as a new method of structural analysis and has been successfully applied to analyze thrust and normal fault systems. However, the restoration of strike- and oblique fault systems using the restoration workflow does not generally recover sufficient amounts of strike-slip, thus leading to unsatisfactory results. In order to better constrain the restoration of such systems, we propose to combine classical boundary conditions with new fault-slip constraints. We investigate several possible sets of constraints by restoring a synthetic balanced model of a restraining bend system that includes a fold above an oblique-slip fault connecting two right-lateral strike-slip faults. The restored geometries and corresponding strain distribution are compared, showing that the best results are obtained by constraining either the walls of the model or the fault line with known gradients of slip. However, when dealing with natural structures where the slip is not known everywhere along the fault, a more realistic approach consists in constraining only piercing points, which also leads to acceptable results.

We then apply this approach to a restraining bend located in the outer fold-and-thrust belt in the deepwater Niger Delta. Although the deformation in the region is largely focused on thrust-fault systems, gradients in the shortening are also accommodated in the northern part of the Delta toe by the development of transport-parallel tear faults. In some locations, steps or relays between tear fault splays result in restraining bend architectures. The high quality of the seismic data in the region allows us to identify and map in detail one of these structures, and to image several channels offsets on the horizons. This provides us fault-slip constraints that are used in our new restoration workflow, yielding an improved assessment of the deformation required to accommodate the tear-faults displacement within the restraining bends.

The use of fault-slip constraints combined with classical boundary conditions offers a realistic approach for using geologic observations to constrain 3D restorations of strike- and oblique slip fault systems, enhancing the effectiveness of these methods in addressing the associated deformation.

Final ID: T51C-2347

Incorporating fault-slip constraints in 3D geomechanical restoration with application to restraining bend systems in the deep-water Niger Delta.

P. Durand-Riard; [1]; *J. H. Shaw;* [1]; *A. Plesch;* [1];

1. Department of Structural Geology and Earth Resources, Harvard University, Cambridge, MA, United States.

Body: In the past few years, geomechanical restoration has emerged as a new method of structural analysis and has been successfully applied to analyze thrust and normal fault systems. However, the restoration of strike- and oblique fault systems using the restoration workflow does not generally recover sufficient amounts of strike-slip, thus leading to unsatisfactory results. In order to better constrain the restoration of such systems, we propose to combine classical boundary conditions with new fault-slip constraints. We investigate several possible sets of constraints by restoring a synthetic balanced model of a restraining bend system that includes a fold above an oblique-slip fault connecting two right-lateral strike-slip faults. The restored geometries and corresponding strain distribution are compared, showing that the best results are obtained by constraining either the walls of the model or the fault line with known gradients of slip. However, when dealing with natural structures where the slip is not known everywhere along the fault, a more realistic approach consists in constraining only piercing points, which also leads to acceptable results.

We then apply this approach to a restraining bend located in the outer fold-and-thrust belt in the deepwater Niger Delta. Although the deformation in the region is largely focused on thrust-fault systems, gradients in the shortening are also accommodated in the northern part of the Delta toe by the development of transport-parallel tear faults. In some locations, steps or relays between tear fault splays result in restraining bend architectures. The high quality of the seismic data in the region allows us to identify and map in detail one of these structures, and to image several channels offsets on the horizons. This provides us fault-slip constraints that are used in our new restoration workflow, yielding an improved assessment of the deformation required to accommodate the tear-faults displacement within the restraining bends.

The use of fault-slip constraints combined with classical boundary conditions offers a realistic approach for using geologic observations to constrain 3D restorations of strike- and oblique slip fault systems, enhancing the effectiveness of these methods in addressing the associated deformation.

Final ID: S51E-02

Radiated Energy of Great Earthquakes

A. Baltay; [1]; *S. Ide;* [2]; *G. C. Beroza;* [1];

1. Stanford University, Stanford, CA, United States.
2. University of Tokyo, Tokyo, Japan.

Body: We investigate the radiated seismic energy of recent great (M_w>*8*) earthquakes that are well recorded by the Global Seismographic Network, including 2011 M_w *9.0* Tohoku, 2010 M_w *8.8* Maule, 2005 M_w *8.7* Nias, and 2007 M_w *8.5* Southern Sumatra earthquakes. We use a teleseismic eGf deconvolution approach to estimate radiated seismic energy, expanding on the method of *Ide et al.* [2011]. Both *P*- and *S*- wave broadband displacement coda records (from 90 s prior to 270 s after the direct arrival) from GSN stations at distances of 30^o to 90^o from the epicenter are analyzed. Smaller events ranging in size from M_w *6.5* to M_w *7.4* and located within ~50 km of the mainshock are used as eGf events. We assume a standard corner frequency and Brune ω^{-2} spectrum for each eGf and correct the main event spectrum accordingly to remove wave propagation effects. We estimate radiated energy from the area under the squared velocity source spectrum.

We use at least 4 different eGf events to analyze each of these great earthquakes, and average the radiated energy from all eGf events and all three components (*P*-wave vertical, *S*-wave radial and transverse). The radiated energy, E_s , of each of the great earthquakes analyzed is very consistent with individual estimates of *Convers and Newman* [2011]. The scaled energy, E_s/M_o , for each of these events is between 1- and $2x10^{-5}$, the same range of scaled energy that is observed for earthquakes over a wide range of sizes, from *M 1.0* to *M 9.0*. This corroborates the fact that scaled energy and apparent stress is constant globally and not dependent on earthquake magnitude. Using *P*-wave vertical, and *S*- wave radial and transverse components yields consistent source spectra and radiated energy estimates, indicating that the eGf deconvolution results in stable and reliable results.

For each of these earthquakes, we find a strong azimuthal dependence of E_s , which we attribute to rupture directivity. In the case of the Tohoku 2011 earthquake, we interpret peaks in the strike direction to be generated by high apparent velocity along the trench.

Events as small as M_w *6.5* have adequate signal-to-noise at teleseismic distances, and thus can be used as eGfs, implying that mainshocks as small as ~*M 8* can be analyzed with this method. We test this with the M_w *7.8* Northern Sumatra earthquake of April 2010 to show that we can estimate energy consistent with that of *Convers and Newman* [2011]. This method can also be adapted to run rapidly or in real time, as potential eGf events can be pre-processed and the analysis run when a new great earthquake occurs. Rapid estimation of radiated energy may be useful for seismic or tsunami hazard warning. Furthermore, the azimuthal energy dependence may quickly inform the rupture model and directivity, which may also aid in rapid hazard characterization.

Final ID: S51E-02

Radiated Energy of Great Earthquakes

A. Baltay; [1]; *S. Ide;* [2]; *G. C. Beroza;* [1];

1. Stanford University, Stanford, CA, United States.
2. University of Tokyo, Tokyo, Japan.

Body: We investigate the radiated seismic energy of recent great (M_w>*8*) earthquakes that are well recorded by the Global Seismographic Network, including 2011 M_w *9.0* Tohoku, 2010 M_w *8.8* Maule, 2005 M_w *8.7* Nias, and 2007 M_w *8.5* Southern Sumatra earthquakes. We use a teleseismic eGf deconvolution approach to estimate radiated seismic energy, expanding on the method of *Ide et al.* [2011]. Both *P*- and *S*- wave broadband displacement coda records (from 90 s prior to 270 s after the direct arrival) from GSN stations at distances of 30^o to 90^o from the epicenter are analyzed. Smaller events ranging in size from M_w *6.5* to M_w *7.4* and located within ~50 km of the mainshock are used as eGf events. We assume a standard corner frequency and Brune ω^{-2} spectrum for each eGf and correct the main event spectrum accordingly to remove wave propagation effects. We estimate radiated energy from the area under the squared velocity source spectrum.

We use at least 4 different eGf events to analyze each of these great earthquakes, and average the radiated energy from all eGf events and all three components (*P*-wave vertical, *S*-wave radial and transverse). The radiated energy, E_s , of each of the great earthquakes analyzed is very consistent with individual estimates of *Convers and Newman* [2011]. The scaled energy, E_s/M_o , for each of these events is between 1- and $2x10^{-5}$, the same range of scaled energy that is observed for earthquakes over a wide range of sizes, from *M 1.0* to *M 9.0*. This corroborates the fact that scaled energy and apparent stress is constant globally and not dependent on earthquake magnitude. Using *P*-wave vertical, and *S*- wave radial and transverse components yields consistent source spectra and radiated energy estimates, indicating that the eGf deconvolution results in stable and reliable results.

For each of these earthquakes, we find a strong azimuthal dependence of E_s , which we attribute to rupture directivity. In the case of the Tohoku 2011 earthquake, we interpret peaks in the strike direction to be generated by high apparent velocity along the trench.

Events as small as M_w *6.5* have adequate signal-to-noise at teleseismic distances, and thus can be used as eGfs, implying that mainshocks as small as ~*M 8* can be analyzed with this method. We test this with the M_w *7.8* Northern Sumatra earthquake of April 2010 to show that we can estimate energy consistent with that of *Convers and Newman* [2011]. This method can also be adapted to run rapidly or in real time, as potential eGf events can be pre-processed and the analysis run when a new great earthquake occurs. Rapid estimation of radiated energy may be useful for seismic or tsunami hazard warning. Furthermore, the azimuthal energy dependence may quickly inform the rupture model and directivity, which may also aid in rapid hazard characterization.

Final ID: S51D-05

Full-3D Waveform Tomography for Southern California

E. Lee; [1]; *P. Chen;* [1]; *T. H. Jordan;* [2]; *P. J. Maechling;* [2]; *M. Denolle;* [3]; *G. C. Beroza;* [3];

1. Geology & Geophysics, University of Wyoming, Laramie, WY, United States.
2. Department of Earth Sciences, University of Southern California, Los Angeles, CA, United States.
3. Department of Geophysics, Stanford University, Stanford, CA, United States.

Body: Our full-3D tomography (F3DT) uses 3D SCEC Community Velocity Model Version 4.0 (CVM4) in Southern California as initial model, a staggered-grid finite-difference code to simulate seismic wave propagation and the sensitivity (Fréchet) kernels are calculated based on the scattering integral and adjoint methods to iteratively improve the model. We use both earthquake recordings and ambient noise Green's function data, stacking of station-to-station correlations of ambient seismic noise, in our F3DT inversions. To reduce errors of earthquake sources, the epicenters and source parameters of earthquakes used in our F3DT are inverted based on full-wave method. In the first two iterations, we used scattering integral to construct sensitivity (Fréchet) kernels of broadband phase-delay measurements and LSQR algorithm to invert 3D perturbations. In first iteration, we only used waveforms from regional earthquakes and the waveforms of updated model generally provide better fit to the observed waveforms. In second iteration, we only used ambient noise Green's function data in inversion and the synthetic waveforms generated by updated model not only improved ambient noise Green's function waveform fittings but also earthquake waveform similarities. Since the waveform fittings of earthquake waveforms and ambient noise Green's function data are improved after first two iterations, we start to combine frequency dependent measurements made on waveforms of earthquake and ambient noise Green's function data and to use adjoint method for structure perturbations. After six iterations, the current model reduced the variance of the waveform misfit more than 55%.

Final ID: S51E-05

Ground Motion Prediction for a scenario M 7 Earthquake on the Southern San Andreas Fault Using the Virtual Source Approach

M. Denolle; [1]; *E. M. Dunham;* [1]; *G. C. Beroza;* [1]; *G. Prieto;* [2];

1. geophysics, stanford, Stanford, CA, United States.
2. Departamento de Física, Universidad de los Andes, Bogotá, Colombia.

Body: The utility of empirical ground motion prediction equations is limited by the scarcity of large events. Physics-based simulations provide an important way to overcome this data scarcity, provided they accurately take into account the complexity of the source, the crustal elastic and anelastic structure and the local site effects. Our incomplete knowledge on crustal structure is an important source of uncertainty in ground motion simulations. We use the ambient seismic field to validate ground motion predictions at long periods. We compute the impulse responses of the Earth in between specific seismic station pairs with ambient seismic field analysis. Comparison of impulse responses with earthquake records from moderate earthquakes confirms that this process preserves relative amplitude. The distribution of the noise sources is not homogeneous, however, and this has the potential to bias amplitude variations. To help overcome this effect, we combine the ambient field results with impulse responses computed from coda-wave interferometry using the aftershock sequence of the April 4th, 2010, M7.2, El Mayor-Cucapah earthquake. We correct the impulse responses with simple analysis on the dispersion of the surface waves to account for the depth-dependence of excitation as well as radiation pattern and directivity effects. We use a spectral collocation method using Chebyshev polynomials to evaluate the depth-dependence of the fundamental mode surface-wave excitation for complex crustal structure. We validate the improved waveform match that results by comparing with moderate earthquakes in southern California. We apply our approach to a temporary seismic network that was deployed along the southern segment of the San Andreas Fault (SAVELA experiment), adding directivity effects using the representation theorem. As predicted by large scale computer simulations strong ground motion amplification in the Los Angeles sedimentary basin is clearly observed in the scenarios we study for a large M7+ strike-slip earthquake on the reach of the San Andreas Fault near San Gorgonio Pass.

Final ID: S52A-01

CISN ShakeAlert: Delivering test warnings for California earthquakes

R. M. Allen; [1]; *M. Boese;* [2]; *H. Brown;* [1]; *M. Caprio;* [3]; *G. B. Cua;* [3]; *M. Fischer;* [3]; *D. D. Given;* [4]; *E. Hauksson;* [2]; *T. H. Heaton;* [2]; *M. Hellweg;* [1]; *I. Henson;* [1]; *M. Liukis;* [5]; *P. J. Maechling;* [5]; *M. A. Meier;* [3]; *D. S. Neuhauser;* [1]; *D. H. Oppenheimer;* [6]; *K. Solanki;* [2];

1. UC Berkeley, Berkeley, CA, United States.
2. Caltech, Pasadena, CA, United States.
3. ETH Zurich, Zurich, Switzerland.
4. US Geological Survey, Pasadena, CA, United States.
5. Southern California Earthquake Center/University Southern California, Los Angeles, CA, United States.
6. US Geological Survey, Menlo Park, CA, United States.

Body: The Earthquake Early Warning (EEW) project team within the California Integrated Seismic Network (CISN) has been developing a test earthquake alerting system for the past five years. The project is a collaboration between Caltech, UC Berkeley, ETH Zurich, USC/SCEC and the USGS, and is funded by the USGS. We use data from the recently upgraded academic- and government-operated geophysical networks across the state to rapidly detect earthquakes and assess the hazard. The test system is operational statewide and delivers warnings to project scientists and other interested scientists. Three event detection and hazard assessment algorithms are currently used: Virtual Seismologist, Onsite and ElarmS, but others may be added to the system. The algorithms provide hazard assessments to a DecisionModule that aggregates the information. It then generates a unified alert stream that is broadcast to certified users. The alerts are received via the UserDisplay, a pop-up computer application. When it opens, the UserDisplay shows a map with the event location and magnitude, and tracks the propagation of the P- and S-waves. It also shows a countdown to shaking at the user's location and an estimate of the expected peak shaking intensity. The algorithm and DecisionModule outputs are archived by the project testing center for independent performance evaluation. Over the coming year the project intends to release alerts to a small group of test users. Identification and engagement of possible project partners is already well underway. Individual project components presentations will provide additional detail.

URL: http://www.cisn.org/eew/

Final ID: S52A-07

Near Real-time Full-wave Centroid Moment Tensor (CMT) Inversion for Ground-motion forecast in 3D Earth Structure of Southern California

E. Lee; [1]; *P. Chen;* [1]; *T. H. Jordan;* [2]; *P. J. Maechling;* [2];

1. Geology & Geophysics, Univ of WY-Geology & Geophys, Laramie, WY, United States.
2. Department of Earth Sciences, University of Southern California, Los Angeles, WY, United States.

Body: Accurate and rapid CMT inversion is important for seismic hazard analysis. We have developed an algorithm for very rapid full-wave CMT inversions in a 3D Earth structure model and applied it on earthquakes recorded by the Southern California Seismic Network (SCSN). The procedure relies on the use of receiver-side Green tensors (RGTs), which comprise the spatial-temporal displacements produced by the three orthogonal unit impulsive point forces acting at the receiver. We have constructed a RGT database for 219 broadband stations in Southern California using an updated version of the 3D SCEC Community Velocity Model (CVM) version 4.0 and a staggered-grid finite-difference code. Finite-difference synthetic seismograms for any earthquake in our modeling volume can be simply calculated by extracting a small, source-centered volume from the RGT database and applying the reciprocity principle. We have developed an automated algorithm that combines a grid-search for suitable epicenter and focal mechanisms with a gradient-descent method that further refines the grid-search results. In this algorithm, the CMT solutions are inverted near real-time by using waveform in a 3D Earth structure. Comparing with the CMT solutions provided by the Southern California Seismic Network (SCSN) shows that our solutions generally provide better fit to the observed waveforms. Our algorithm may provide more robust CMT solutions for earthquakes in Southern California. In addition, the rapid and accurate full-wave CMT inversion has potential to extent to accurate near real-time ground-motion prediction based on 3D structure model for earthquake early warning purpose. When combined with real-time telemetered waveform recordings, our algorithm can provide (near) real-time ground-motion forecast.

Final ID: S52B-06

Broadband Ground Motion Simulations for a Kinematic Variation of the Mw 7.8 ShakeOut Rupture

R. W. Graves; [1]; *E. Seyhan;* [2]; *J. P. Stewart;* [2];

1. US Geological Survey, Pasadena, CA, United States.
2. Civil & Environmental Engineering, UCLA, Los Angeles, CA, United States.

Body: The 2008 ShakeOut Scenario (Porter et al., 2011) describes a hypothetical Mw 7.8 earthquake on the southern San Andreas Fault, the associated simulated ground motions, and their potential impact on the built environment. The main features of the rupture scenario, including its end-points, magnitude, and gross slip distribution, were defined through expert opinion. Other details of the original rupture description such as slip at smaller length scales, rupture speed, and rise time were constrained using empirical relationships and experience gained from previous strong-motion modeling (Hudnut et al., 2008). Subsequent analyses considering the sensitivity of kinematically prescribed rupture speed (Graves et al., 2008) and fully spontaneous dynamic rupture parameterizations (Olsen et al., 2009) found that ground motion amplification due to rupture directivity can be significantly affected by the coherency of the rupture across the fault surface. Here, we build on these earlier studies by considering an alternative kinematic parameterization of the ShakeOut rupture developed using the methodology presented by Graves and Pitarka (2010). The resulting rupture description has a high degree of spatial and temporal complexity, which leads to a reduction in the coherence of the radiated energy and diminished longer period rupture directivity effects relative to the original scenario. Analysis of the original ShakeOut results by Star et al. (2011) also found the shorter period simulations attenuate faster with distance and have lower intra-event sigma compared with empirical predictions. We have addressed these issues by adjusting the Q value used in the model and increasing the stochastic variability in the shorter period simulation approach. Comparison of the updated simulation results with estimates from ground motion prediction equations shows improved distance attenuation behavior and an intra-event dispersion that is similar to the empirical models at periods longer than about 1 sec, and closer to, but still somewhat lower, at shorter periods.

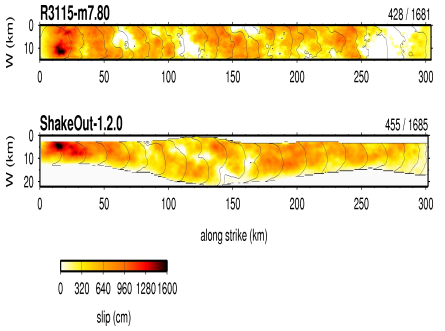

Comparison of slip distribution and rupture propagation contours for updated (top) and original (bottom) kinematic ShakeOut models. The updated model exhibits stronger heterogeneity in both slip and rupture evolution.

Final ID: S53A-2255

Development of ShakeAlert Performance Evaluation Software

P. J. Maechling; [1]; *M. Liukis;* [1]; *T. H. Jordan;* [1];

1. University of Southern California, Southern California Earthquake Center, Los Angeles, CA, United States.

Body: The CISN Testing Center (CTC) is designed to provide automated and interactive performance evaluations of ShakeAlert earthquake early warning system performance. The CTC software consists of two main parts: (1) software programs that input ShakeAlert EEW performance reports, match ShakeAlert forecasts to observational data, and generate a variety of EEW system performance summaries, and (2) an automated testing framework that can input ShakeAlert EEW performance reports, retrieve ANSS observational data, and produce performance summaries on a daily, or event, basis. The interactive capabilities of the CTC software may be useful for offline testing of ShakeAlert system. The automated capabilities of the CTC software are designed to support ongoing ShakeAlert performance evaluations. The CTC software implements a number of standard EEW performance summaries including magnitude forecast error and location forecast error with evaluation of ShakeAlert ground motion forecasts such as peak velocity under development. The CTC software is distributed as open-source scientific software to support transparency in evaluation processing and to support testing software re-use within ShakeAlert development groups.
URL: http://www.scec.org/eew

Final ID: T53C-04

Active blind-thrust faulting and growth folding in the southern Longmen Shan, eastern Tibetan Plateau

M. Wang; [1]; *D. Jia;* [1]; *J. H. Shaw;* [2]; *A. Lin;* [3]; *B. Liu;* [4]; *Y. Li;* [1];

1. Department of Earth Sciences, Nanjing University, Nanjing, China.
2. Department of Earth and Planetary Sciences, Harvard University, Cambridge, MA, United States.
3. Graduate School of Science and Technology, Shizuoka University, Shizuoka, Japan.
4. Geophysical Exploration Center, China Earthquake Administration, Zhengzhou, China.

Body: The devastating 2008 Wenchuan earthquake demonstrates that the central and northern parts of the Longmen Shan fold-and-thrust belt are currently active. However, geological evidences of active faulting and folding in the unruptured southern Longmen Shan remain poorly determined. We define the activity of the Qiongxi thrust fault system (QTF) along the south Longmen Shan range front by integrating deep & shallow seismic reflection data, geomorphic observations, and trench survey. The QTF is a 50-km-long, NS-trending set of faults that exhibit geomorphic evidence of late Quaternary surface deformation. Trench survey and radiocarbon ages reveal that a recent surface rupturing event occurred in the past 2420±40 BP on a set of steeply east-dipping faults that are part of this system. 3D structural modeling reveals that these faults are backthrusts that merge at depth with the blind, west-dipping QTF ramp. This blind thrust ramp accommodates east-west shortening and is overlain by fault-bend folds. Growth strata above the QTF include discrete zones of dipping strata with well-defined axial surfaces, indicating that fold growth has occurred during deposition of the late Pliocene-Quaternary strata. The trend and sense of reverse slip along the QTF indicates that the structure accommodates east-west crustal shortening of the south Longmen Shan and reflects the growth of eastern Tibetan Plateau in the late Cenozoic. This shortening direction is consistent with the oblique, right-lateral reverse rupture on faults that trend northeast-southwest during the Wenchuan earthquake. This study also demonstrates that the QTF has generated a sizeable earthquake in the Holocene, and thus should be considered in future seismic hazard assessments of the southern Longmen Shan and densely populated western Sichuan basin.

Final ID: S54C-07

Effect of Sediments on Rupture Dynamics of Shallow Subduction Zone Earthquakes and Tsunami Generation

S. Ma; [1];

1. San Diego State University, San Diego, CA, United States.

Body: Low-velocity fault zones have long been recognized for crustal earthquakes by using fault-zone trapped waves and geodetic observations on land. However, the most pronounced low-velocity fault zones are probably in the subduction zones where sediments on the seafloor are being continuously subducted. In this study I focus on shallow subduction zone earthquakes; these earthquakes pose a serious threat to human society in their ability in generating large tsunamis. Numerous observations indicate that these earthquakes have unusually long rupture durations, low rupture velocities, and/or small stress drops near the trench. However, the underlying physics is unclear. I will use dynamic rupture simulations with a finite-element method to investigate the dynamic stress evolution on faults induced by both sediments and free surface, and its relations with rupture velocity and slip. I will also explore the effect of off-fault yielding of sediments on the rupture characteristics and seafloor deformation. As shown in Ma and Beroza (2008), the more compliant hanging wall combined with free surface greatly increases the strength drop and slip near the trench. Sediments in the subduction zone likely have a significant role in the rupture dynamics of shallow subduction zone earthquakes and tsunami generation.